The stochastic organization of genomes and
the doctrine of energy-information evolution based on bio-antenna arrays

Sergey V. Petoukhov

Mechanical Engineering Research Institute of Russian Academy of Sciences. Russia, 101990, Moscow, M. Kharitonievskiy pereulok, 4, http://eng.imash.ru/, info@imash.ru

Comment: Some materials of this article were presented by the author in his keynote speech at the International Symmetry Festival-2021 (Sophia, Bulgaria, 9-12 July 2021, https://festival.symmetry.hu/) and in his speeches at the Seventh International Conference in Code Biology (Lužnica, Croatia, 31 August – 4 September 2021, https://www.codebiology.org/conferences/Luznica2021/), at the Fifth International Conference of Artificial Intelligence, Medical Engineering, Education (Moscow, Russia, 1-3 October 2021, http://www.icics.net/conf/2021/AIMEE2021/index.html), and at the International Interdisciplinary Medical Congress of Natural Medicine (19-20 March, Slovak Republic, https://www.acuclinic.eu/, online).

Abstract. The article continues the author's publications about the matrix-tensor study of universal rules of stochastic (probabilistic) organization of long single-stranded DNA sequences in eukaryotic and prokaryotic genomes. The author reveals that corresponding matrices of probabilities of n-plets in n-textual representations of each genomic DNA are numerically interrelated each with other in such algebraic form, which has analogies with formalisms of the known tensor-matrix theory of digital antenna arrays. These arrays combine many separate antennas into a single coordinated ensemble with unique emergent properties, due to which antenna arrays are widely used in devices of medicine, astrophysics, avionics, etc. The noted analogies allow putting forward the author's hypothesis that the stochastic organization of genomic DNAs is connected with bio-antenna arrays. From the point of view of this hypothesis, many known facts about using principles of antenna arrays in inherited physiological phenomena are collected in a single grouping with genomic DNAs. This new topic about the biological meaning of profitable properties of antenna arrays includes problems of biological evolution, the origin of the genetic code, regenerative medicine, and the development of algebraic biology. These issues are discussed jointly with the author's results of quantum information analysis of stochastic features of genomic DNAs.

Keywords: genomic DNA, probability, matrices, tensor product, Hadamard product, antenna arrays, photonic crystals, liquid crystals, biophotonics, quantum informatics

Contents

1. Introduction

This article continues a description of the author's results, which add to his previously published ones, of studying universal rules and symmetries in structures of long single-stranded DNA sequences in eukaryotic and prokaryotic genomes. In his previous publications [Petoukhov, 2008, 2022a-c], the author presented the tensor family of genetic matrices $[C, A; T, G]^{(n)}$, each of which combines all members of one of the n-plets4 alphabets of DNA: the alphabet of 4 nucleotides C, A, T, G; the alphabet of 16 duplets; the alphabets of 64 triplets, etc. (Fig. 1.1). Here (n) is a tensor power.

	0	1
0	C	A
1	T	G

	00	01	10	11
00	CC	CA	AC	AA
01	CT	CG	AT	AG
10	TC	TA	GC	GA
11	TT	TG	GT	GG

	000	001	010	011	100	101	110	111
000	CCC	CCA	CAC	CAA	ACC	ACA	AAC	AAA
001	CCT	CCG	CAT	CAG	ACT	ACG	AAT	AAG
010	CTC	CTA	CGC	CGA	ATC	ATA	AGC	AGA
011	CTT	CTG	CGT	CGG	ATT	ATG	AGT	AGG
100	TCC	TCA	TAC	TAA	GCC	GCA	GAC	GAA
101	TCT	TCG	TAT	TAG	GCT	GCG	GAT	GAG
110	TTC	TTA	TGC	TGA	GTC	GTA	GGC	GGA
111	TTT	TTG	TGT	TGG	GTT	GTG	GGT	GGG

	0000	0001	0010	0011	0100	0101	0110	0111	1000	1001	1010	1011	1100	1101	1110	1111
0000	CCCC	CCCA	CCAC	CCAA	CACC	CACA	CAAC	CAAA	ACCC	ACCA	ACAC	ACAA	AACC	AACA	AAAC	AAAA
0001	CCCT	CCCG	CCAT	CCAG	CACT	CACG	CAAT	CAAG	ACCT	ACCG	ACAT	ACAG	AACT	AACG	AAAT	AAAG
0010	CCTC	CCTA	CCGC	CCGA	CATC	CATA	CAGC	CAGA	ACTC	ACTA	ACGC	ACGA	AATC	AATA	AAGC	AAGA
0011	CCTT	CCTG	CCGT	CCGG	CATT	CATG	CAGT	CAGG	ACTT	ACTG	ACGT	ACGG	AATT	AATG	AAGT	AAGG
0100	CTCC	CTCA	CTAC	CTAA	CGCC	CGCA	CGAC	CGAA	ATCC	ATCA	ATAC	ATAA	AGCC	AGCA	AGAC	AGAA
0101	CTCT	CTCG	CTAT	CTAG	CGCT	CGCG	CGAT	CGAG	ATCT	ATCG	ATAT	ATAG	AGCT	AGCG	AGAT	AGAG
0110	CTTC	CTTA	CTGC	CTGA	CGTC	CGTA	CGGC	CGGA	ATTC	ATTA	ATGC	ATGA	AGTC	AGTA	AGGC	AGGA
0111	CTTT	CTTG	CTGT	CTGG	CGTT	CGTG	CGGT	CGGG	ATTT	ATTG	ATGT	ATGG	AGTT	AGTG	AGGT	AGGG
1000	TCCC	TCCA	TCAC	TCAA	TACC	TACA	TAAC	TAAA	GCCC	GCCA	GCAC	GCAA	GACC	GACA	GAAC	GAAA
1001	TCCT	TCCG	TCAT	TCAG	TACT	TACG	TAAT	TAAG	GCCT	GCCG	GCAT	GCAG	GACT	GACG	GAAT	GAAG
1010	TCTC	TCTA	TCGC	TCGA	TATC	TATA	TAGC	TAGA	GCTC	GCTA	GCGC	GCGA	GATC	GATA	GAGC	GAGA
1011	TCTT	TCTG	TCGT	TCGG	TATT	TATG	TAGT	TAGG	GCTT	GCTG	GCGT	GCGG	GATT	GATG	GAGT	GAGG
1100	TTCC	TTCA	TTAC	TTAA	TGCC	TGCA	TGAC	TGAA	GTCC	GTCA	GTAC	GTAA	GGCC	GGCA	GGAC	GGAA
1101	TTCT	TTCG	TTAT	TTAG	TGCT	TGCG	TGAT	TGAG	GTCT	GTCG	GTAT	GTAG	GGCT	GGCG	GGAT	GGAG
1110	TTTC	TTTA	TTGC	TTGA	TGTC	TGTA	TGGC	TGGA	GTTC	GTTA	GTGC	GTGA	GGTC	GGTA	GGGC	GGGA
1111	TTTT	TTTG	TTGT	TTGG	TGTT	TGTG	TGGT	TGGG	GTTT	GTTG	GTGT	GTGG	GGTT	GGTG	GGGT	GGGG

Fig. 1.**1**. The first members of the tensor family of matrices [C, A; T, G]$^{(n)}$ present the DNA alphabets of 4 nucleotides, 16 duplets, 64 triplets, and 256 tetraplets.

In Fig. 1.1, the columns and rows of the matrices of DNA alphabets are enumerated by binary numbers based on the following binary-oppositional molecular features of nucleotides: the columns are numbered due to binary indicators "pyrimidine-or-purine" (C=T=0, A=G=1), and the rows are numbered due to binary indicators "amino-or-keto" (C=A=0, T=G=1). For example, the triplet CAT belongs to column number 010 and row number 001, since its nucleotide sequence in terms of these indicators is: "pyrimidine-purine-pyrimidine" and "amino-amino-keto".

It is convenient for us for further description to show at the first position of each of the nucleotides its binary symbol from the second pair of binary-oppositional indicators (the indicator "amino or keto": C=A=0, T=G=1) and at the second positions of each of the letters its binary symbol from the first pair of binary-oppositional indicators (the indicator "pyrimidine or purine": C=T=0, A=G=1). In this case, the letter C is represented by the binary symbol 00 (that is, as a 2-bit binary number), A – by the symbol 01, T – by the symbol 10, and G – by the symbol 11. Using these representations of separate letters, each of 16 doublets is represented as a concatenation of the binary symbols of its letters (that is aa s 4-bit binary number): for example, the doublet CC is represented as 4-bit binary number 0000, the doublet CA – as 4-bit binary number 0001, etc. By analogy, each of the 64 triplets is represented as a concatenation of the binary symbols of its letters (that is as a 6-bit binary number): for example, the triplet CCC is represented as 6-bit binary number 000000, the triplet CCA – as 6-bit binary number 000001, etc.

Taking into account a set of the DNA n-plets alphabets (like in Fig. 1.1), each DNA sequence can be considered not as a separate information text but as a set (or a bunch) of many parallel DNA texts, each of which is written in one of these n-plets alphabets (in other words, in this approach, any DNA sequence is presented as a bunch of parallel messages in different alphabets). For example, the DNA sequence ACCTGTAACG... is a bunch of the following texts, which we briefly term as n-texts of the DNA:

- a 1-text of nucleotides (A-C-C-C-T-G- ...);
- a 2-text of doublets (AC-CT-GT-AA-CG- ...);
- a 3-text of triplets (ACC-TGT-AAC- ..); etc.

In each of such different n-texts of the same long DNA sequence, one can calculate the percentages of each of its n-plets and then compare sets of calculated percentages from different n-texts. This comparative analysis of a wide set of eukaryotic and prokaryotic genomes revealed hidden algebraic interrelations among percentage compositions of these genomic n-texts and allowed the formulation of fundamental rules of stochastic organizations of the genomes [Petoukhov, 2020a-c, 2021a]. The revealed rules give pieces of evidence of the existence of global-genomic algebraic invariants, which remain unchanged over millions of years of biological evolution, during which millions of species of organisms die and new ones arise (although locally genomic sequences are modified under the action of mutations, the pressing of natural selection, etc.).

To show new results in this article, the author uses some data from previous articles [Petoukhov, 2020a-c, 2021a,b]. First of all, this is matrices of percentages of n-plets in different n-texts of DNA of the human chromosome №1 (Figs. 1.2-1.4), in

which each of the n-plets from symbolic matrices in Fig. 1.1 is replaced by its percent value in the corresponding n-text of this DNA. Binary numerations of columns and rows are conserved. Percents are shown in fractions of one, and their values are rounded. Initial data on the chromosome were taken in the GenBank: https://www.ncbi.nlm.nih.gov/nuccore/NC_000001.11.

	0	1
0	%C	%A
1	%T	%G

$\rightarrow \quad P_1 =$

	0	1
0	0.208499	0.291001
1	0.291756	0.208744

	00	01	10	11
00	%CC	%CA	%AC	%AA
01	%CT	%CG	%AT	%AG
10	%TC	%TA	%GC	%GA
11	%TT	%TG	%GT	%GG

$\rightarrow \quad P_2 =$

	00	01	10	11
00	0.054090	0.072739	0.050327	0.095037
01	0.071341	0.010305	0.074290	0.071368
10	0.060080	0.063123	0.044024	0.060083
11	0.095680	0.072859	0.050459	0.054195

Fig. 1.2. The left matrices contain percentage symbols of 4 monoplets and 16 duplets with the same locations of these n-plets as in corresponding matrices in Fig. 1.1. The right matrices P_1 and P_2 show percentage values of all monoplets and duplets correspondingly in the 1-text and 2-text representations of the DNA nucleotide sequence of the human chromosome №1.

	000	001	010	011	100	101	110	111
000	%CCC	%CCA	%CAC	%CAA	%ACC	%ACA	%AAC	%AAA
001	%CCT	%CCG	%CAT	%CAG	%ACT	%ACG	%AAT	%AAG
010	%CTC	%CTA	%CGC	%CGA	%ATC	%ATA	%AGC	%AGA
011	%CTT	%CTG	%CGT	%CGG	%ATT	%ATG	%AGT	%AGG
100	%TCC	%TCA	%TAC	%TAA	%GCC	%GCA	%GAC	%GAA
101	%TCT	%TCG	%TAT	%TAG	%GCT	%GCG	%GAT	%GAG
110	%TTC	%TTA	%TGC	%TGA	%GTC	%GTA	%GGC	%GGA
111	%TTT	%TTG	%TGT	%TGG	%GTT	%GTG	%GGT	%GGG

$\rightarrow$

$P_3 =$

	000	001	010	011	100	101	110	111
000	0.013845	0.018782	0.015236	0.018615	0.011825	0.019768	0.014466	0.036928
001	0.018532	0.002906	0.017889	0.021037	0.016224	0.002537	0.023753	0.019875
010	0.017584	0.012749	0.002508	0.002272	0.013175	0.019420	0.014406	0.022369
011	0.020088	0.020880	0.002591	0.002911	0.023881	0.017807	0.016136	0.018480
100	0.015877	0.019642	0.011031	0.019859	0.012545	0.014563	0.009615	0.019596
101	0.022258	0.002330	0.019392	0.012844	0.014374	0.002531	0.013271	0.017560
110	0.019724	0.019810	0.014573	0.019469	0.009561	0.011152	0.012560	0.015998
111	0.037246	0.018843	0.019881	0.018954	0.014452	0.015337	0.011855	0.013822

Fig. 1.3. The upper matrix contains percentage symbols of 64 triplets with the same location as in the corresponding (8*8)-matrix in Fig. 1.1. The bottom matrix P_3 shows percentage values of all triplets in the 3-text representation of the DNA nucleotide sequence of the human chromosome №1.

$P_4 =$

	0000	0001	0010	0011	0100	0101	0110	0111	1000	1001	1010	1011	1100	1101	1110	1111
0000	.0033	.0055	.0042	.0044	.0040	.0056	.0032	.0070	.0030	.0042	.0040	.0053	.0032	.0059	.0055	.0149
0001	.0041	.0010	.0044	.0058	.0047	.0010	.0040	.0044	.0041	.0005	.0051	.0054	.0047	.0006	.0095	.0071
0010	.0050	.0029	.0008	.0006	.0036	.0039	.0049	.0059	.0037	.0032	.0006	.0006	.0040	.0070	.0037	.0066
0011	.0048	.0058	.0006	.0009	.0057	.0047	.0045	.0058	.0049	.0044	.0007	.0007	.0071	.0057	.0049	.0047
0100	.0052	.0057	.0027	.0038	.0010	.0006	.0003	.0006	.0033	.0045	.0032	.0063	.0042	.0049	.0039	.0078
0101	.0058	.0009	.0035	.0028	.0007	.0003	.0005	.0008	.0049	.0005	.0064	.0035	.0046	.0007	.0049	.0059
0110	.0048	.0036	.0046	.0051	.0005	.0004	.0008	.0006	.0047	.0056	.0033	.0050	.0031	.0037	.0047	.0057
0111	.0073	.0044	.0053	.0058	.0006	.0010	.0005	.0010	.0096	.0040	.0051	.0044	.0046	.0047	.0040	.0041
1000	.0046	.0049	.0042	.0051	.0024	.0045	.0028	.0078	.0030	.0041	.0029	.0038	.0023	.0037	.0029	.0073
1001	.0057	.0006	.0051	.0052	.0037	.0004	.0056	.0036	.0047	.0008	.0033	.0046	.0030	.0005	.0046	.0048
1010	.0057	.0040	.0005	.0006	.0030	.0055	.0026	.0041	.0032	.0027	.0006	.0005	.0025	.0031	.0032	.0057
1011	.0068	.0058	.0006	.0006	.0070	.0039	.0032	.0029	.0037	.0048	.0006	.0008	.0041	.0036	.0036	.0051
1100	.0051	.0063	.0034	.0063	.0041	.0049	.0031	.0061	.0023	.0031	.0017	.0035	.0031	.0042	.0023	.0052
1101	.0077	.0006	.0063	.0038	.0049	.0006	.0045	.0057	.0038	.0004	.0032	.0027	.0042	.0010	.0034	.0052
1110	.0073	.0078	.0038	.0051	.0037	.0046	.0042	.0051	.0030	.0028	.0029	.0042	.0023	.0024	.0030	.0046
1111	.0150	.0072	.0055	.0045	.0059	.0057	.0043	.0054	.0055	.0032	.0040	.0042	.0032	.0039	.0030	.0033

Fig. 1.4. The matrix P_4 shows percentage values of all 256 tetraplets in the 4-text representation of the DNA nucleotide sequence of the human chromosome №1. The location of these values corresponds to the location of tetraplets in the (16*16)-matrix in Fig. 1.1.

At first glance, the set of values in the percentage matrices (Figs. 1.2-1.4) is quite chaotic. It has the following features regarding the percent of separate *n*-plets:

- Percent of presented *n*-plets significantly depends on the order of letters in them. For example, the percent of doublets CG and GC, having the same letter composition, differ several times: %CG = 0.0103, and %GC = 0.0440;
- The numerical percent matrices for doublets, triplets, and tetraplets (Figs. 1.2-1.4) are not tensor powers of the nucleotide percent (2*2)-matrix (Fig. 1.2).

But in fact, these matrices are naturally interconnected, which will be discussed below.

The main aim of this article is the following:

1) Describe revealed system analogies between matrices, which are used in the theory of digital antenna arrays, and percentage matrices of universal stochastic organization of DNA sequences in eukaryotic and prokaryotic genomes from publications [Petoukhov, 2020b,c, 2021a] (like in Figs. 1.2-1.4);

2) Present the first application of algebraic matrix operations from the theory of digital antenna arrays to model numeric interconnections inside families of mentioned percent matrices of n-texts of genomic DNAs;

3) Show the first materials of the author's doctrine about the key role of mathematics of the digital bio-antenna arrays and their wave functions (including radiation patterns) for understanding the evolutionary phenomena of self-organization of living bodies, which are based on wave energy-information intercommunication among their components.

With the presented approach, biological evolution is considered as the evolution of systems of digital bio-antenna arrays (or gratings) and their interrelated wave multipath radiations, providing energy-information communication of body parts with each other and with the outside world.6 From the point of view of this doctrine, energy-information communication orientation appears in evolution, which can be considered as an important system-forming factor of biological essences.

2. System analogies between genomic percentage matrices and matrices in the theory of digital antenna arrays

Is there a meaningful algebraic-matrix relationship of a typical kind between

the phenomenological probability matrices $\mathbf{P_1}$, $\mathbf{P_2}$, $\mathbf{P_3}$, and $\mathbf{P_4}$ (Figs. 1.2-1.4)? Yes, such a relationship exists. Its revealing shows important probability properties of stochastic organization of genomic DNAs, which lead to perspective ideas about a connection of genomic DNAs with the theory of digital antenna arrays and also with formalisms of quantum informatics. Let us explain this.

The number of members in the n-plets alphabet of DNA is 4^{n-1}. Accordingly, when passing from the n-plets alphabet to the (n+1)-plets alphabet, which is represented in the same tensor family of matrices $[C, A; T, G]^{(n)}$ (Fig. 1.1), the number of alphabetic members becomes 4 times more. This tensor multiplication of any n-plet by the (2*2)-matrix [C, A; T, G] associates with each n-plet from the first alphabet four n+1-plets of the second alphabet, that is, it is an operation of tetra-multiplicating (or tetra-breeding) of alphabetic members in this transition to the next alphabet.

To simplify the explanation, let us consider in more detail the case of the relationship between the percentage of 4 monoplets in the 1-text representation of genomic DNA and the percentage of 16 duplets in its 2-text representation. In this case, for example, each of the 4 monoplets C, A, T, G turns out to be associated - through the tensor product of matrices - immediately with four corresponding duplets shown on the right side of expressions (2.1):

$$
\begin{aligned}
[C] \otimes [C, A; T, G] &= [CC, CA; CT, CG], \\
[A] \otimes [C, A; T, G] &= [AC, AA; AT, AG], \\
[T] \otimes [C, A; T, G] &= [TC, TA; TT, TG], \\
[G] \otimes [C, A; T, G] &= [GC, GA; GT, GG].
\end{aligned}
\qquad (2.1)
$$

Concerning the relationships between the named percentages of 4 monoplets and 16 duplets, we accept by analogy the following: the percentage matrix of each of the quadruples of doublets indicated in (2.1) is the result of the tensor product of the percentage matrices of monoplets [%C], [%A], [%T], [%G] by the corresponding (2*2)-matrices with unknown real coefficients following expressions (2.2) and (2.3):

$$
\begin{aligned}
[\%C] \otimes [B_C] &= [\%CC, \%CA; \%CT, \%CG]), \\
[\%A] \otimes [B_A] &= [\%AC, \%AA; \%AT, \%AG]), \\
[\%T] \otimes [B_T] &= [\%TC, \%TA; \%TT, \%TG]), \\
[\%G] \otimes [B_G] &= [\%GC, \%GA; \%GT, \%GG])
\end{aligned}
\qquad (2.2)
$$

where

$$
\begin{aligned}
B_C &= [b_{C00}, b_{C01}; b_{C10}, b_{C11}], \quad & B_A &= [b_{A00}, b_{A01}; b_{A10}, b_{A11}], \\
B_T &= [b_{T00}, b_{T01}; b_{T10}, b_{T11}], \quad & B_G &= [b_{G00}, b_{G01}; b_{G19}, b_{G11}]
\end{aligned}
\qquad (2.3)
$$

These matrices B_C, B_A, B_T, B_G (2.3) map the percentage of each nucleotide to the percentage of four duplets, and therefore they are conditionally called tetra-multiplicating matrices. From (2.2) and (2.3), one can derive the expressions for the named 16 coefficients in terms of the ratios of the percentages of the corresponding duplets and monoplets:

$[\%C*b_{C00}, \%C*b_{C01}; \%C*b_{C10}, \%C*b_{C11}] = [\%CC, \%CA; \%CT, \%CG]) \rightarrow$
$\rightarrow b_{C00} = \%CC / \%C, \quad b_{C01} = \%CA / \%C, \quad b_{C10} = \%CT / \%C, \quad b_{C11} = \%CG / \%C;$

$[\%A*b_{A00}, \%A*b_{A01}; \%A*b_{A10}, \%A*b_{A11}] = [\%AC, \%AA; \%AT, \%AG]) \rightarrow$

$\rightarrow b_{A00} = \%AC / \%A,\ b_{A01} = \%AA / \%A,\ b_{A10} = \%AT / \%A,\ b_{A11} = \%AG / \%A;$

$[\%T*b_{T00}, \%T*b_{T01}; \%T*b_{T10}, \%T*b_{T11}] = [\%TC, \%TA; \%TT, \%TG]) \rightarrow$
$\rightarrow b_{T00} = \%TC / \%T,\ b_{T01} = \%TA / \%T,\ b_{T10} = \%TT / \%T,\ b_{T11} = \%TG / \%T;$

$[\%G*b_{G00}, \%G*b_{G01}; \%G*b_{G10}, \%G*b_{G11}] = [\%GC, \%GA; \%GT, \%GG]) \rightarrow$
$\rightarrow b_{G00}=\%GC / \%G,\ b_{G01}=\%GA / \%G,\ b_{G10}=\%GT / \%G,\ b_{G11}=\%GG / \%G$ (2.4)

We need to algebraically express the system connection between the entire percentage (2*2)-matrix of 4 monoplets [%C, %A; %T, %G] and the percentage (4*4)-matrix of 16 duplets (see the symbolic matrix in Fig. 1.2 on the left). This can be done using an algebraic operation called the Hadamard product for matrices, which is indirectly related to the tensor product. The Hadamard product is known in the theory of digital antenna arrays, artificial intelligence, and many other areas of matrix analysis of systems. We will use the Hadamard product due to the convenience of expressing the desired matrix relationships with it, as well as the usefulness of the emerging associations between the matrix representations of genetic systems and the matrix representations of other systems, primarily in the theory of digital antenna arrays.

The Hadamard product (also known as the element-wise product, entrywise product, or Schur product [Horn, Johnson, 2012]) is a binary operation that takes two matrices of the same dimensions and produces another matrix of the same dimension as the operands, where each element *i, j* is the product of elements *i, j* of the original two matrices. In other words, for two matrices *A* and *B* of the same dimension $m \times n$, the Hadamard product $A \odot B$ is a matrix of the same dimension as the operands, with elements given by $(A \odot B)_{ij} = (A)_{ij}(B)_{ij}$. The symbol $\odot$ denotes the Hadamard product. The expression (2.5) shows an example of the Hadamard product for two (2*2)-matrices:

$$\begin{vmatrix} a_{00}, a_{01} \\ a_{10}, a_{11} \end{vmatrix} \odot \begin{vmatrix} b_{00}, b_{01} \\ b_{10}, b_{11} \end{vmatrix} = \begin{vmatrix} a_{00}b_{00},\ a_{01}b_{01} \\ a_{10}b_{10},\ a_{11}b_{11} \end{vmatrix} \qquad (2.5)$$

The Hadamard product is a principal submatrix of the tensor (or Kronecker) product [Günther, Klotz, 2012].

Fig. 2.1 shows the Hadamard product of two (2*2) matrices, in the second of which the entries B_C, B_A, B_T, B_G are tetra-multiplicating (2*2)-matrices with real coefficients from expressions (2.3). On the whole, the second matrix appears as a colony or a union of 4 tetra-multiplicating matrices. This Hadamard product of two matrices (shown in Fig. 2.1, top) defines a percentage matrix of 16 duplets (Figure 2.1, bottom)

$$\begin{vmatrix} \%C, \%A \\ \%T, \%G \end{vmatrix} \odot \begin{vmatrix} B_C, B_A \\ B_T, B_G \end{vmatrix} = \begin{vmatrix} \%C*B_C, \%A*B_A \\ \%T*B_T,\ \%G*B_G \end{vmatrix} =$$

$$=$$

%CC	%CA	%AC	%AA
%CT	%CG	%AT	%AG
%TC	%TA	%GC	%GA
%TT	%TG	%GT	%GG

Fig. 2.1. Representation of the 16-duplet percent matrix (shown at bottom) via the Hadamard product of the monoplet percent (2*2)-matrix with the block (2*2)-matrix, in which the entries B_C, B_A, B_T, B_G are (2*2)-matrices from (2.3) with the coefficients defined in the expression (2.4).

Now let's move from the general symbolic expression of the relationship of percentage matrices of 4 monoplets and 16 duplets (Fig. 2.1) to the analysis of the numeric relationship of phenomenological percentages in the concrete case of DNA of human chromosome No. 1 (from Fig. 1.2). In this case, symbolic expressions (2.3) and (2.4) give the numeric tetra-multiplicating matrices shown in Fig. 2.2. Each of them contains 4 real numbers, which can be interpreted as percentages in fractions of one (their values are rounded here to 6 decimal places).

$$B_C = \begin{array}{|c|c|} \hline 0.054090 / 0.208499 & 0.072739 / 0.208499 \\ \hline 0.071341 / 0.208499 & 0.010305 / 0.208499 \\ \hline \end{array} = \begin{array}{|c|c|} \hline 0.259426 & 0.348870 \\ \hline 0.342165 & 0.049425 \\ \hline \end{array}$$

$$B_A = \begin{array}{|c|c|} \hline 0.050327 / 0.291001 & 0.095037 / 0.291001 \\ \hline 0.074290 / 0.291001 & 0.071368 / 0.291001 \\ \hline \end{array} = \begin{array}{|c|c|} \hline 0.172944 & 0.326587 \\ \hline 0.255291 & 0.245250 \\ \hline \end{array}$$

$$B_T = \begin{array}{|c|c|} \hline 0.060080 / 0.291756 & 0.063123 / 0.291756 \\ \hline 0.095680 / 0.291756 & 0.072859 / 0.291756 \\ \hline \end{array} = \begin{array}{|c|c|} \hline 0.205925 & 0.216355 \\ \hline 0.327945 & 0.249726 \\ \hline \end{array}$$

$$B_G = \begin{array}{|c|c|} \hline 0.044024 / 0.208744 & 0.060083 / 0.208744 \\ \hline 0.050459 / 0.208744 & 0.054195 / 0.208744 \\ \hline \end{array} = \begin{array}{|c|c|} \hline 0.210899 & 0.287831 \\ \hline 0.241727 & 0.259624 \\ \hline \end{array}$$

Fig. 2.2. Tetra-multiplicating matrices from expressions (2.3) and (2.4) in the case of DNA of human chromosome №1.

Fig. 2.2 shows that the tetra-multiplicating matrices B_C, B_A, B_T, and B_G differ significantly from each other in their sets of numerical entries. But at the same time, as it turns out, they obey the general rule: the sum of all entries in each of these matrices is equal to 1 (accurate to the third decimal place) (Fig. 2.3). This rule adds to the list of genetic gestalt rules, in which the value of the sum practically does not change with a wide variability of the summand values [Petoukhov, 2021a].

Matrix	Sum of matrix entries
B_C	0.259426 + 0.348870 + 0.342165 + 0.049425 = **0.999886**
B_A	0.172944 + 0.326587 + 0.255291 + 0.245250 = **1.000072**
B_T	0.205925 + 0.216355 + 0.327945 + 0.249726 = **0.999951**
B_G	0.210899 + 0.287831 + 0.241727 + 0.259624 = **1.000081**

$$\begin{array}{|c|c|} \hline B_C & B_A \\ \hline B_T & B_G \\ \hline \end{array} \;\;\rightarrow\;\; \begin{array}{|c|c|} \hline 0.999886 & 1.000072 \\ \hline 0.999951 & 1.000081 \\ \hline \end{array}$$

Fig. 2.3. Equality to the unity of the sum of all the 4 entries in each of the tetra-multiplicating matrices B_C, B_A, B_T, B_G in the case of DNA of human chromosome №1. Top: different summands give practically the same sums in each of these

matrices. Bottom: an additional visual presentation of this colony of matrices B_C, B_A, B_T, B_G and their corresponding sums of entries.

In the DNA of different genomes, the sets of entries in the tetra-multiplicating matrices B_C, B_A, B_T, and B_G can be significantly different. But the unit sum rule for all four entries in different tetra-multiplicating matrices B_C, B_A, B_T, B_G (represented by a particular example in Fig. 2.3) is universal and holds for the entire wide range of eukaryotic and prokaryotic genomes studied by the author [Petoukhov, 2019-2021].

Taking into account the equalities (2.4) and the unit sum rule (Fig. 2.3), calculations of sums of 4 entries in each of the (2*2)-quadrants of the (4*4)-matrix give the following:

$$\%CC + \%CA + \%CT + \%CG = \%C*(b_{C00} + b_{C01} + b_{C10} + b_{C11}) \approx \%C,$$
$$\%AC + \%AA + \%AT + \%AG = \%A*(b_{A00} + b_{A01} + b_{A10} + b_{A11}) \approx \%A,$$
$$\%TC + \%TA + \%TT + \%TG = \%T*(b_{T00} + b_{T01} + b_{T10} + b_{T11}) \approx \%T,$$
$$\%GC + \%GA + \%GT + \%GG = \%G*(b_{G00} + b_{G01} + b_{G10} + b_{G11}) \approx \%G \qquad (2.5)$$

The expressions (2.5) correspond to the universal phenomenological rule of genomic DNA previously described by the author [Petoukhov, 2019-2021] and are represented by expressions: $\%C \approx \Sigma\%CN$, $\%A \approx \Sigma\%AN$, $\%T \approx \Sigma\%TN$, $\%G \approx \Sigma\%GN$, where N denotes any of the nucleotides C, A, T, G.

In connection with the author's previous publications on the relationship of DNA alphabets with the formalisms of quantum informatics [Petoukhov, 2021a; Petoukhov, Petukhova, Svirin, 2019], we especially note the following. The four entries of each tetra-multiplicating matrix B_C, B_A, B_T, B_G, giving the unit sum, can be considered as probabilities in a two-qubit quantum system, which is traditionally expressed as follows in Dirac notations [Nielsen, Chuang, 2010, p.16]:

$$|\psi_{12}> = \alpha_{00}|00> + \alpha_{01}|01> + \alpha_{10}|10> + \alpha_{11}|11> \qquad (2.6)$$

In (2.6), the coefficients α_{00}, α_{01}, α_{10}, α_{11} are called the probability amplitudes of the corresponding computational basis states $|00>$, $|01>$, $|10>$, $|11>$. They satisfy the normalization condition for probabilities (2.7):

$$\alpha_{00}^2 + \alpha_{01}^2 + \alpha_{10}^2 + \alpha_{11}^2 = 1, \qquad (2.7)$$

which is associated with the indicated unit sum rule of genomes (Fig. 2.3). Some interesting connections between the stochastic organization of genomic DNAs and formalisms of quantum informatics are described in this article below.

One can note also that - in the case of the considered genomic DNA – numeric tetra-multiplicating matrices B_C, B_A, B_T, and B_G are not completely independent of each other but their entries are interrelated by some relations. Fig. 2.4 shows the colonial union of these 4 matrices into a single (4*4)-matrix using data from Fig. 2.2. In this colonial (4*4)-matrix, the sums of the entries in rows (as well as in columns), which are located symmetrically, are approximately equal.

B_C	B_A		0.259427	0.348870	0.172945	0.326585	1.107827
B_T	B_G	=	0.342167	0.049426	0.255290	0.245251	0.892135
			0.205927	0.216354	0.210899	0.287829	0.921009
			0.327944	0.249727	0.241725	0.259624	1.079021
			1.135465	0.864378	0.880859	1.119288	

Fig. 2.4. The colonial (4*4)-matrix combines 4 tetra-multiplicating (2*2)-matrices B_C, B_A, B_T, B_G. The numeric data taken from Fig. 2.2 in the case of DNA of human chromosome №1 are shown. Sums of entries in each of the columns are marked by yellow, and sums of entries in each of the rows are marked by blue.

Let us now turn to the algebraic relationship between the percentage (4*4)-matrix of 16 duplets and the percentage (8*8)-matrix of 64 triplets (Fig. 1.3 and 1.4). Fig. 2.5 shows this relationship via the Hadamard product by analogy with Fig. 2.1.

%CC	%CA	%AC	%AA
%CT	%CG	%AC	%AG
%TC	%TA	%GC	%GA
%TT	%TG	%GT	%GG

○

B_{CC}	B_{CA}	B_{AC}	B_{AA}
B_{CT}	B_{CG}	B_{AT}	B_{AG}
B_{TC}	B_{TA}	B_{GC}	B_{GA}
B_{TT}	B_{TG}	B_{GT}	B_{GG}

=

%CCC	%CCA	%CAC	%CAA	%ACC	%ACA	%AAC	%AAA
%CCT	%CCG	%CAT	%CAG	%ACT	%ACG	%AAT	%AAG
%CTC	%CTA	%CGC	%CGA	%ATC	%ATA	%AGC	%AGA
%CTT	%CTG	%CGT	%CGG	%ATT	%ATG	%AGT	%AGG
%TCC	%TCA	%TAC	%TAA	%GCC	%GCA	%GAC	%GAA
%TCT	%TCG	%TAT	%TAG	%GCT	%GCG	%GAT	%GAG
%TTC	%TTA	%TGC	%TGA	%GTC	%GTA	%GGC	%GGA
%TTT	%TTG	%TGT	%TGG	%GTT	%GTG	%GGT	%GGG

Fig. 2.5. Representation of the 64-triplet percent matrix (shown at bottom) via the Hadamard product of the duplet percent (4*4)-matrix with the block (4*4)-matrix, whose 16 entries B_{CC}, B_{CA}, B_{CG}, B_{CG}, B_{AC}, B_{AA}, B_{AT}, B_{AG}, B_{CC}, B_{CA}, B_{CT}, B_{CG}, B_{GC}, B_{GA}, B_{GT}, B_{GG} are tetra-multiplicating (2*2)-matrices from Fig. 2.6.

Tetra-multiplicating matrices in Fig. 2.5 are defined by analogy with the previous case shown in expression (2.4). Fig. 2.6 presents these 16 tetra-multiplicating matrices, whose entries are equal to ratios of percent of corresponding triplets and duplets shown in Figs. 1.2 and 1.3.

B_{CC} =

%CCC / %CC	%CCA / %CC
%CCT / %CC	%CCG / %CC

; B_{CA} =

%CAC / %CA	%CAA / %CA
%CAT / %CA	%CAG / %CA

B_{AC} =

%ACC / %AC	%ACA / %AC
%ACT / %AC	%ACG / %AC

; B_{AA} =

%AAC / %AA	%AAA / %AA
%AAT / %AA	%AAG / %AA

B_{CT} =

%CTC / %CT	%CTA / %CT
%CTT / %CT	%CTG / %CT

; B_{CG} =

%CGC / %CG	%CGA / %CG
%CGT / %CG	%CGG / %CG

$$
B_{AT} = \begin{array}{|c|c|} \hline \%ATC\,/\,\%AT & \%ATA\,/\,\%AT \\ \hline \%ATT\,/\,\%AT & \%ATG\,/\,\%AT \\ \hline \end{array} \quad ; \quad B_{AG} = \begin{array}{|c|c|} \hline \%AGC\,/\,\%AG & \%AGA\,/\,\%AG \\ \hline \%AGT\,/\,\%AG & \%AGG\,/\,\%AG \\ \hline \end{array}
$$

$$
B_{TC} = \begin{array}{|c|c|} \hline \%TCC\,/\,\%TC & \%TCA\,/\,\%TC \\ \hline \%TCT\,/\,\%TC & \%TCG\,/\,\%TC \\ \hline \end{array} \quad ; \quad B_{TA} = \begin{array}{|c|c|} \hline \%TAC\,/\,\%TA & \%TAA\,/\,\%TA \\ \hline \%TAT\,/\,\%TA & \%TAG\,/\,\%TA \\ \hline \end{array}
$$

$$
B_{GC} = \begin{array}{|c|c|} \hline \%GCC\,/\,\%GC & \%GCA\,/\,\%GC \\ \hline \%GCT\,/\,\%GC & \%GCG\,/\,\%GC \\ \hline \end{array} \quad ; \quad B_{GA} = \begin{array}{|c|c|} \hline \%GAC\,/\,\%GA & \%GAA\,/\,\%GA \\ \hline \%GAT\,/\,\%GA & \%GAG\,/\,\%GA \\ \hline \end{array}
$$

$$
B_{TT} = \begin{array}{|c|c|} \hline \%TTC\,/\,\%TT & \%TTA\,/\,\%TT \\ \hline \%TTT\,/\,\%TT & \%TTG\,/\,\%TT \\ \hline \end{array} \quad ; \quad B_{TG} = \begin{array}{|c|c|} \hline \%TGC\,/\,\%TG & \%TGA\,/\,\%TG \\ \hline \%TGT\,/\,\%TG & \%TGG\,/\,\%TG \\ \hline \end{array}
$$

$$
B_{GT} = \begin{array}{|c|c|} \hline \%GTC\,/\,\%GT & \%GTA\,/\,\%GT \\ \hline \%GTT\,/\,\%GT & \%GTG\,/\,\%GT \\ \hline \end{array} \quad ; \quad B_{GG} = \begin{array}{|c|c|} \hline \%GGC\,/\,\%GG & \%GGA\,/\,\%GG \\ \hline \%GGT\,/\,\%GG & \%GGG\,/\,\%GG \\ \hline \end{array}
$$

Fig. 2.6. 16 symbolic tetra-multiplicating matrices noted in Fig. 2.5, whose entries are equal to ratios of percent of corresponding triplets and duplets shown in Figs. 1.2 and 1.3.

In the concrete case of percentages in 2-texts and 3-texts of DNA of human chromosome №1 (represented in Figs. 1.2 and 1.3), the tetra-multiplicating matrices from Fig. 2.6 get the numeric forms shown in Fig. 2.7.

$$
B_{CC} = \begin{array}{|c|c|} \hline 0.255962 & 0.347236 \\ \hline 0.342614 & 0.053725 \\ \hline \end{array} \quad ; \quad B_{CA} = \begin{array}{|c|c|} \hline 0.209464 & 0.255911 \\ \hline 0.245935 & 0.289207 \\ \hline \end{array}
$$

$$
B_{AC} = \begin{array}{|c|c|} \hline 0.234964 & 0.392793 \\ \hline 0.322369 & 0.050406 \\ \hline \end{array} \quad ; \quad B_{AA} = \begin{array}{|c|c|} \hline 0.152210 & 0.388563 \\ \hline 0.249937 & 0.209134 \\ \hline \end{array}
$$

$$
B_{CT} = \begin{array}{|c|c|} \hline 0.246475 & 0.178701 \\ \hline 0.281582 & 0.292675 \\ \hline \end{array} \quad ; \quad B_{CG} = \begin{array}{|c|c|} \hline 0.243414 & 0.220494 \\ \hline 0.251465 & 0.282438 \\ \hline \end{array}
$$

$$
B_{AT} = \begin{array}{|c|c|} \hline 0.177344 & 0.261409 \\ \hline 0.321454 & 0.239696 \\ \hline \end{array} \quad ; \quad B_{AG} = \begin{array}{|c|c|} \hline 0.201857 & 0.313426 \\ \hline 0.226093 & 0.258937 \\ \hline \end{array}
$$

$$
B_{TC} = \begin{array}{|c|c|} \hline 0.264259 & 0.326923 \\ \hline 0.370469 & 0.038782 \\ \hline \end{array} \quad ; \quad B_{TA} = \begin{array}{|c|c|} \hline 0.174753 & 0.314608 \\ \hline 0.307214 & 0.203470 \\ \hline \end{array}
$$

$$
B_{GC} = \begin{array}{|c|c|} \hline 0.284965 & 0.330797 \\ \hline 0.326511 & 0.057502 \\ \hline \end{array} \quad ; \quad B_{GA} = \begin{array}{|c|c|} \hline 0.160038 & 0.326148 \\ \hline 0.220872 & 0.292257 \\ \hline \end{array}
$$

$$
B_{TT} = \begin{array}{|c|c|} \hline 0.206149 & 0.207045 \\ \hline 0.389283 & 0.196943 \\ \hline \end{array} \quad ; \quad B_{TG} = \begin{array}{|c|c|} \hline 0.200019 & 0.267209 \\ \hline 0.272874 & 0.260144 \\ \hline \end{array}
$$

$$
B_{GT} = \begin{array}{|c|c|} \hline 0.189482 & 0.221009 \\ \hline 0.286418 & 0.303943 \\ \hline \end{array} \quad ; \quad B_{GG} = \begin{array}{|c|c|} \hline 0.231754 & 0.295197 \\ \hline 0.218745 & 0.255051 \\ \hline \end{array}
$$

Fig. 2.7. Tetra-multiplicating matrices from Fig. 2.6 in the case of numeric data of DNA of human chromosome №1.

The sum of all 4 entries in each of these 16 tetra-multiplicating matrices in Figs. 2.5-2.7 is equal to 1 (accurate to the second decimal place) (Fig. 2.8).

B_{CC}	B_{CA}	B_{AC}	B_{AA}
B_{CT}	B_{CG}	B_{AT}	B_{AG}
B_{TC}	B_{TA}	B_{GC}	B_{GA}
B_{TT}	B_{TG}	B_{GT}	B_{GG}

➔

0.9995	1.0005	1.0005	0.9998
0.9994	0.9978	0.9999	1.0003
1.0004	1.0000	0.9998	0.9993
0.9994	1.0002	1.0009	1.0007

Fig. 2.8. **At left**: symbols of the 16 tetra-multiplicating (2*2)-matrices from Figs. 2.5-2.7. **At right**: a matrix of corresponding sums of 4 entries in these (2*2)-matrices; each of these sums is equal to 1 with high-level precision.

It is this unit sum rule that determines, in particular, the universal phenomenological rule of genomic DNA previously described by the author [Petoukhov, 2019-2021] and represented in expression (2.8) by some analogy with expression (2.5):

%CC ≈ Σ %CCN, %CA ≈ Σ %CAN, %CT ≈ Σ %CTN, %CG ≈ Σ %CGN,
%AC ≈ Σ %ACN, %AA ≈ Σ %AAN, %AT ≈ Σ %ATN, %AG ≈ Σ %AGN,
%TC ≈ Σ %TCN, %TA ≈ Σ %TAN, %TT ≈ Σ %TTN, %TG ≈ Σ %TGN,
%GC ≈ Σ %GCN, %GA ≈ Σ %GAN, %GT ≈ Σ %GTN, %GG ≈ Σ %GGN,   (2.8)
where N denotes any of the nucleotides C, A, T, and G.

In the case of the considered genomic DNA, 16 numeric tetra-multiplicating matrices from Fig. 2.2 are not completely independent of each other but their entries are interrelated by some additional relations. Fig. 2.9 shows the colonial union of these 16 matrices into a single (8*8)-matrix using data from Fig. 2.7. In this colonial (8*8)-matrix, the sums of the entries in rows (as well as in columns), which are located symmetrically, are approximately equal (by analogy with the previous case in Fig. 2.4).

B_{CC}	B_{CA}	B_{AC}	B_{AA}
B_{CT}	B_{CG}	B_{AT}	B_{AG}
B_{TC}	B_{TA}	B_{GC}	B_{GA}
B_{TT}	B_{TG}	B_{GT}	B_{GG}

=

0.255962	0.347227	0.209464	0.255911	0.234964	0.392793	0.152210	0.388563	2.237094
0.342613	0.053731	0.245935	0.289207	0.322369	0.050406	0.249937	0.209134	1.763331
0.246475	0.178701	0.243414	0.220494	0.177344	0.261409	0.201857	0.313426	1.843119
0.281582	0.292675	0.251465	0.282438	0.321454	0.239696	0.226093	0.258937	2.154341
0.264259	0.326923	0.174753	0.314608	0.284965	0.330797	0.160038	0.326148	2.182491
0.370469	0.038782	0.307214	0.203470	0.326511	0.057502	0.220872	0.292257	1.817077
0.206149	0.207045	0.200019	0.267209	0.189482	0.221009	0.231754	0.295197	1.817864
0.389283	0.196943	0.272874	0.260144	0.286418	0.303943	0.218745	0.255051	2.183400
2.356791	1.642028	1.905139	2.093480	2.143507	1.857555	1.661505	2.338713	

Fig. 2.9. The colonial (8*8)-matrix, which combines 16 tetra-multiplicating (2*2)-matrices from Figs. 2.5 and 2.7. The numeric data taken from Fig. 2.7 in the case of DNA of human chromosome №1 are shown. Sums of entries in each of the columns are marked by yellow, and sums of entries in each of the rows are marked by blue.

Such chain of algebraic relationships - using the Hadamard product like in Figs. 2.1 and 2.5 - between the percentage (2^n*2^n)-matrices of 4^n n-plets and the percentage $(2^{n+1}*2^{n+1})$-matrices of 4^{n+1} (n+1)-plets can be continued by analogy for cases n = 4, 5, 6, … (but n should be much smaller the length of genomic DNA).

It should be additionally noted that the same matrix representation based on the Hadamard product of matrices (like in Figs. 2.1, 2.5) is appropriate for the stochastic organization of n-texts in so-called epi-chains of genomic DNAs; the study of epi-chains gave pieces of evidence regarding the fractal-like stochastic organization of genomic DNAs [Petoukhov, 2019, 2021a]. By definition, in a nucleotide sequence N_1 of any DNA strand N_1 (Fig. 2.10a) with sequentially numbered nucleotides 1, 2, 3, 4, ..., epi-chains of different orders k are such sparse subsequences that contain only those nucleotides, whose numeration differ from each other by natural number $k = 1$, 2, 3, 4, … Fig. 2.10 shows some schematic examples of DNA epi-chains of different orders.
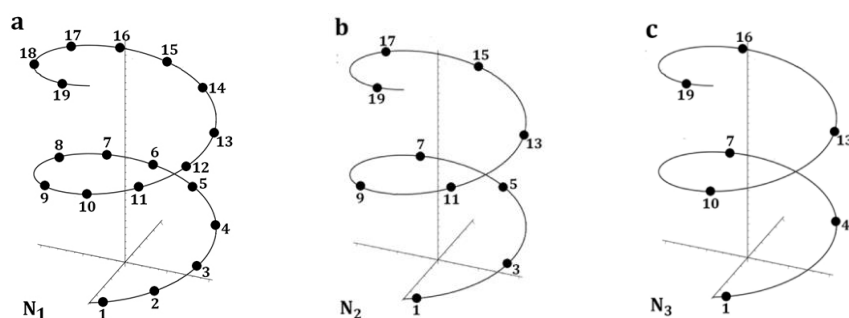
Fig. 2.10. Schematic representations of a single-stranded DNA and its initial epi-chains of numerated nucleotides, denoted by black circles. **a**, a sequence N_1 of numerated nucleotides of the DNA strand; **b**, an epi-chain of the second-order N_2 having nucleotides with numbers 1-3-5-7-…; **c**, an epi-chain of the third-order N_3 nucleotides numbers 1-4-7-10-… . (from [Petoukhov, 2021]).

The matrix-tensor results described in this section lead to new approaches in two important scientific fields:

1) usage of analogies between matrix genetics [Petoukhov, 2008, 2019-2021] and tensor-matrix theory of digital antenna arrays, where using the Hadamard product for matrices provides a huge profit in calculations and synthesis of high-effective antenna arrays (or grids) [Slyusar, 1999; Minochkin, Rudakov, Slyusar, 2011, p. 442].

In this field, the author develops his doctrine of energy-information biological evolution based on multi-level interrelated bio-antenna arrays providing multi-beam radiation and absorption of wave energy and information, and also possessing properties of self-organization and development in ontogenesis and phylogenesis;

2) modeling molecular-genetic structures and universal stochastics rules of genomic DNAs based on formalisms of quantum informatics [Petoukhov, 2021a; Petoukhov, Petukhova, Svirin, 2019; etc.].

The next sections of the article describe these approaches in more detail.

3. The doctrine of energy-information evolution based on bio-antenna arrays and their wave functioning

The method of revealing analogies is one of the basic methods of development of sciences, where it plays an important heuristic role, as it is known at least from the time of B.Bolzano. Max Planck wrote: «*We thus find that it is a characteristic of every new idea occurring in science that it combines in a certain original manner two distinct series of facts*» [Planck, 1936].

On the whole, this section presents the author's doctrine of energy-information evolution based on multi-level interrelated bio-antenna arrays and their wave functioning. This doctrine was generated, firstly, by non-trivial analogies between tensor-matrix descriptions in matrix genetics and the theory of digital antenna arrays, and, secondly, by many facts on the importance of emission and absorption of wave energy and signals by using bio-antenna arrays in genetically inherited physiological systems. From the point of view of this doctrine, DNA informatics uses molecular bio-antenna arrays, whose wave functioning is coordinated with other genetically inherited macro-physiological bio-antenna arrays providing in living bodies many hereditary physiological structures and processes related to emission and absorption of wave energy and signals: compound faceted eyes in insects; inherited photonic-crystal arrays determining species patterns on butterfly wings and other animal bodies; the innate ability to echolocation in animals; and others. Some of these inherited phenomena are connected with intelligent actions of living bodies; for this reason, the proposed doctrine includes the preposition that inherited intelligent abilities of organisms are closely related to the functioning of multi-level bio-antenna arrays, studying of which can lead to new approaches in the creation of artificial intelligence. Below some of these inherited phenomena and their relations to engineering technologies of digital antenna arrays are represented in more detail.

In his famous book "What is Life?", Schrodinger made the auspicious proposal that the genetic material is an "aperiodic crystal" [Schrödinger, 1944; Ball, 2014]. The described author's doctrine of energy-informational evolution continues this line of thought but significantly supplements it with the provision of the key role of bio-antenna arrays and their wave functioning. The doctrine proposes to consider DNA and RNA as a germinal aperiodic crystal of bio-antenna arrays, which serves as a crystallization seed for the aperiodic crystallization of the entire developing organism as a huge growing set of bio-antenna arrays interrelated with each other. The processes of this aperiodic crystallization of the inherited body can be modified under the influence of the environment, nutritional conditions, stages of onto- and phylogenetic development, etc. The functioning of these developing bio-antenna arrays is accompanied by exchanges of wave energy and signals among physiological subsystems and external sources and also by related processes of biological self-organization with the participation of resonances mechanisms and principles of energy minimization. The doctrine considers bio-antenna arrays and their wave functioning as the key element of energy-information evolution, which deserve special attention and study (for brevity, this doctrine can also be called the doctrine of bio-antenna evolution).

This Section represents a set of facts and arguments supporting the described author's doctrine. To start this presentation, let us briefly remind basic facts about digital antenna arrays and their tensor-matrix theory in engineering technologies.

- 3.1. Regarding antenna arrays and matrix approaches in their theory

Modern technology is saturated with antenna arrays of various types, including medical ultrasound scanning technology (on multichannel platforms with digital emitter arrays), sonar systems, radio relay stations, radio astronomic devices, etc. Their importance has led to the intensive development of the mathematical theory of transmitting and receiving antenna arrays of various types, which is presented in many publications. This developing mathematical theory provides new, previously unknown means of matrix-tensor analysis not only for antenna technology but also for mathematical natural science [Minochkin, Rudakov, Slyusar, 2011]. In particular, the author productively uses elements of this matrix-tensor analysis (including the Hadamard product of matrices) in his genetic research.

Fig. 3.1.1. Examples of engineering antenna arrays (taken from https://commons.wikimedia.org/wiki/File:PAK_FA_AESA_maks2009.jpg and https://commons.wikimedia.org/wiki/File:Traqueur_acquisition.JPG, permission is granted to copy, distribute and/or modify these documents under the terms of the GNU Free Documentation License).

Antenna arrays consist of many separate antennas, each of which can emit or absorb waves of a specific frequency range (Fig. 3.1.1). These sets of antennas in antenna arrays can be located in space in a variety of ways on the cylindrical, conical, spiral, and other surfaces periodically, non-equidistantly, quasi-randomly concerning each other, etc. The dimensions of engineering antenna arrays can vary greatly depending on the purpose: from giant arrays in radio astronomy and radio relay stations to nanoantenna arrays, with which modern science associates the development of new types of computer technology (photonics) and energy. The design of nanoantenna arrays can be associated with photonic crystals and liquid crystals, which are actively used in modern technology and which are realized for millions of years in genetically inherited physiological structures, which will be discussed in more detail below. The mathematical description of the operation of engineering antenna arrays operating to emit or receive waves is almost the same.

Antenna arrays are used to provide such kinds of radiation patterns (or beamforming, or spatial filtering), which are unable for a single antenna element (these are emergence properties of antenna arrays). Let's list some of them in line with the book [Voskresensky et al., 2006]. The directivity of the action of the simplest

separate antenna - a symmetrical vibrator - is low. To increase the direction of action, already at the first stages of the development of antenna technology, they began to use a system of vibrators - antenna arrays. Currently, antenna arrays are the most common class of antennas due to the following reasons, the knowledge of which is important for understanding and studying the role of bio-antenna arrays in living organisms:

- An array of N elements allows to increase approximately N times the directivity and, accordingly, the gain of the antenna compared to a single radiator, as well as to narrow the beam to improve the accuracy of determining the angular coordinates of the radiation source in navigation, radar, and other radio systems. With the help of antenna arrays, it is possible to raise the dielectric strength of the antenna and increase the level of radiated (or received) power;

- Antenna arrays are a unique tool for providing communication noise-immunity and extracting a weak signal from a strong noise. For this reason, they are used, for example, in satellite communications technology in navigation satellite systems GPS, GLONASS, Galileo, where the corresponding unique property of antenna arrays to overcome natural noises or special jammings is characterized by the following citation: "*Low power of the received satellite navigation signals leads to situations when jamming of natural or artificial origin, commensurable in power with the wanted signal, may present a danger for navigation communications integrity. In the case of receiving navigation signals against the background of powerful electromagnetic jamming, a substantial increase of signal-to-jamming ratio can only be achieved by way of spatial filtration of signals through the application of antenna arrays*" [Ryapolov, Fambulov, 2018]. This special property of antenna arrays is especially important for understanding the well-known phenomenal ability of organisms to work with weak information signals against a background of strong noise, providing communication noise immunity. The same property of antenna arrays allows us to rethink the amazing noise immunity of genetic coding, as well as the multichannel nature of genetic inheritance, expressed by Mendel's law of independent inheritance of traits (this is discussed below in one of the paragraphs);

- An important advantage of antenna arrays is the ability to quickly (inertialess) survey space by swinging the beam or swinging the antenna by electrical methods (electrical scanning), as well as the possibility of parallel using many beams with their operating at different frequencies and other characteristics. The antenna system is a necessary link to ensure the noise immunity of the radio system, taking into account adaptation to the interference environment.

Given these unique emergent properties of antenna arrays, it can be expected that organisms are forced to use them in their life activity. The doctrine stated in this article confirms this expectation on a set of examples of the structure and functioning of inherited physiological systems based on antenna arrays and their energy wave. We continue the theme of the features of antenna arrays.

An important class of antenna arrays is phased antenna arrays capable of operating with multi-beam radiation patterns (Fig. 3.1.2). A phased array usually means an electronically scanned and computer-controlled array of antennas, which creates a beam of radio waves that can be electronically steered to point in different directions without moving the antennas [Milligan, 2005; Stutzman, Thiele, 2012].
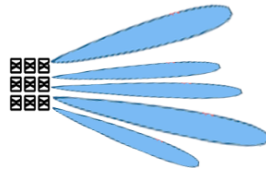
Fig. 3.1.2. A conditional radiation pattern (beamforming) of a multibeam digital antenna array (this image is drawn by the author).

In simple antenna arrays, the radiofrequency current from the transmitter is fed to the individual antenna elements with a differential phase relationship so that the energy from the separate elements adds together to increase the far-field power in the desired direction and suppress radiation in undesired directions (due to wave interference). In other words, the specificity of a phased array antenna is that the amplitude-phase distribution among elements is not fixed, it can be adjusted (changed in a controlled manner) during operation. Thanks to this, it is possible to move the beams of the antenna array in certain sectors of space without mechanical rotations of the antenna. Since the size of an antenna array must extend many wavelengths to achieve high gain, phased arrays are mainly practical at the high-frequency end of the radio spectrum (usually between 300 MHz and 300 GHz). Phased arrays have spread to civilian applications such as 5G MIMO for cell phones. The phased array principle is also used in acoustics for medical ultrasound imaging scanners, oil and gas prospecting, etc.

The operation of antenna arrays is associated not only with the transmission and reception of information signals but also with the reception and transmission of energy. For example, there are rectennas (rectifying antenna [https://en.wikipedia.org/wiki/Rectenna]), which are non-linear antennas designed to convert the field energy of an electromagnetic wave incident on them into direct current energy. The simplest design option can be a half-wave vibrator, between the arms of which a device with one-way conduction (for example, a diode) is installed. To increase the gain, such engineering devices are combined into multi-element arrays. In engineering, rectens are considered promising for energy transmission over long distances, for example, when transporting energy to Earth from solar power plants in space orbit. In living bodies, to pump the energy of electromagnetic waves through possible biological rectens, semiconductors are needed, and they are present in them: "... *almost all types of living organisms are capable of biosynthesis of inorganic compounds, which by their nature are inorganic semiconductors and exhibit photochemical activity*" [Nikandrov, 2000].

The defining feature of the new generation of radio engineering systems is the implementation of their antenna devices using the technology of digital antenna arrays (phased and others), which are often called Smart Antenna or Intelligent Antenna [Minochkin, Rudakov, Slyusar, 2011; Slyusar, 1999]. These arrays additionally use analog-to-digital and digital-to-analog conversions to digitize the wave messages emitted or received by the antenna array to computer process these digital representations of antenna information with various mathematical algorithms to achieve certain goals. Such antenna arrays can operate in a multipath mode with several partial radiation patterns almost simultaneously existing. In particular, smart antennas are used in numerous systems of radio holography, which is an analog of optical holography and uses mathematical matrices for calculating and designing antenna arrays (see, for example, [Pavelyev et al., 2004; Voskresensky et al., 2015; Sazonov, 2015]). In the active digital antenna arrays, the radar transmitter is

distributed ("smeared") over the antenna array and is one of the most reliable elements: if several solid-state modules break down, there is no significant reduction in performance (previously for radars with a passive array, if the transmitter elements came out of the ensemble, the system is "blind").

It is in Smart Antennas that matrix methods are a key tool for the rational synthesis of antenna arrays, as well as the development of effective algorithms for computer processing of digital antenna information and digital beamforming with high noise immunity.

The problems arising here about Smart Antennas, sometimes containing hundreds and thousands of information processing channels, have led to the development of new tools for matrix analysis that have not previously been encountered in other areas of science and technology. First of all, we are talking about the tensor-matrix theory of antenna arrays by the Ukrainian scientist V. Slyusar, who proposed some new operations with matrices (a list of his thematic publications is on [https://en.wikipedia.org/wiki/Vadym_Slyusar]). These new operations in the theory of digital antenna arrays (Smart Antennas) are closely related to the Hadamard product of matrices, which, as shown above, turned out to be adequate for describing the universal rules for the stochastic organization of genomic DNA (Fig. 2.1, 2.5). In technics, the apparatus of the tensor-matrix theory of antenna arrays makes it possible to simplify computational processes "*by replacing the inversion of the multidimensional matrix product (P*P)-1 with an identical procedure for more simply formed Hadamard products…*" [Minochkin, Rudakov, Slyusar, 2011, p. 441-442]. The huge savings in computational costs when using the Hadamard product for matrices in the theory of digital antenna arrays is illustrated by the following citation: «*Calculating the quadratic form by identity is reduced to the Hadamard product. As a result, for a 32x32 antenna array in each channel with 32 synthesized frequency filters in 32 distance intervals, we can decrease the amount of multiplication by 8,004 times and the number of summations by 8,456 times concerning the initial notation. In this case, the number of multiplication operations is decreased by more than 268.845 billion, as compared to a four-coordinate model based on a traditional matrix product*» [Slyusar, 1999, page10; Minochkin, Rudakov, Slyusar, page 442].

Similar matrix methods associated with the Hadamard product for matrices are used in artificial intelligence systems, machine learning, reducing the number of calculations when implementing the tensor sketch method to reduce the data dimension, etc.

- 3.2. Inherited physiological phenomena and the genetic doctrine of energy-informational evolution based on bio-antenna arrays

As noted above, the method of analogies is one of the main methods for the development of science. It was also shown above that the Hadamard product for matrices, which is effectively used in the tensor-matrix theory of digital antenna arrays, unexpectedly showed its involvement in matrix representations of the universal rules for the stochastic organization of genomic DNAs. In short, the tensor-matrix formalisms in DNA informatics turned out to be similar to the formalisms of the tensor-matrix theory of digital antenna arrays.

This gave rise to the author's initial ideas of the stated doctrine of evolution based on bio-antenna arrays and their wave functioning. In this case, we are talking primarily about electromagnetic radiation. But mechanical and electrical oscillations in living bodies are closely connected because many tissues are piezo-electrical

(nucleic acids, actin, dentin, tendons, bone, etc.). The mathematics of mechanical and electrical oscillations is analogical (so-called "electro-mechanical analogies" are well-known). The article [Petoukhov, 2016] describes some aspects of this theme related to resonance phenomena.

It should be mentioned that the concept of resonances plays a fundamental and interdisciplinary role in science. In classic mechanics, the concept of resonances has wide theoretical and engineering applications due to vibrational phenomena of a resonant synchronization of oscillatory processes, vibrational separation and structuring of multiphase systems, Vibro-transportation of substances, Vibro-transmission of energy within systems, etc. [Blekhman, 2000; Ganiev et al., 2015]. Virtually invisible vibrations can give rise to paradoxical phenomena that give the impression of violating the laws of mechanics (it's not for nothing that the article about these phenomena is figuratively called: "*Vibration "changes the laws of mechanics"*" [Blekhman, 2003]. These phenomena include, for example, the following: the upper position of the inverted pendulum becomes stable; a heavy metal ball "floats up" in a layer of sand; a rope takes a form of a vertical stem if a corresponding vibration acts on its base. Inside fluids, vibrating bodies can attract or repel each other (vibrating forces of Bjerknes) and pulsating gas bubbles may coalesce or divide (such phenomena of Vibro-mechanics can explain many processes in living bodies, including complex processes under mitosis and meiosis of cells).

Let us describe some of the inherited physiological phenomena that are included in this doctrine as its natural components due to the following:

- these phenomena are associated with the mechanisms of generation and reception of multicomponent wave radiation, whose parameters are specific to different types of organisms and are inherited from generation to generation;

- they can be explained naturally based on the idea of the energy-information functioning of bio-antenna arrays with their multi-beam radiation patterns.

- 3.2.1. Complex faceted eyes of insects as receiving bio-antenna arrays

Insects, crustaceans, and some other invertebrates receive visual information about the world around them, which is necessary for solving many vital tasks of an intellectual nature (search for food, escape from predators, etc.), through complex faceted eyes. These eyes serve as bio-antenna arrays (grids, or lattices) for receiving electromagnetic waves of the corresponding frequency range. They are formed by special structural units - ommatidia, the corneal lens of which has the form of a convex hexagon - facets. The compound eyes of insects are motionless, located on the sides of the head, and can occupy almost the entire surface of the head. The image perceived by such eyes is "recalculated" from the numerous ommatidia, which point in slightly different directions. The eyes of various insect species consist of a large number of ommatidia: a worker ant has about 100, a housefly has about 4,000, a worker bee has 5,000, butterflies have up to 17,000, and dragonflies have up to 30,000. Fig. 3.2.1.1 shows examples of complex faceted eyes, which serve for receiving electromagnetic waves and have structures similar to engineering antenna arrays.

Fig. 3.2.1.1. Examples of complex faceted eyes. **At left**: compound eye of Antarctic krill as imaged by an electron microscope (from https://en.wikipedia.org/wiki/Compound_eye, photo by Gerd Alberti and Uwe Kils; permission is granted to copy and distribute this document under the terms of the GNU Free Documentation License). **In middle**: Dragonfly compound eyes (from https://en.wikipedia.org/wiki/File:Dragonfly_eye_3811.jpg, author David L. Green; permission is granted to copy and distribute under the Creative Commons Attribution-Share Alike 3.0 Unported license). **At right**: insect compound eye diagram (from https://tftwiki.ru/wiki/Arthropod_eye. Permission is granted to copy, distribute and/or modify this document under the terms of the GNU Free Documentation License, Version 1.2, or any later version published by the Free Software Foundation).

Compound eyes provide a large angular field of vision since the small "elementary eyes" - ommatidia are directed in different directions and can cover a huge angular field up to a full sphere. The compound eye can quickly detect movement since its temporal inertia is 15 times less than that of the human eye. It should also be noted the uniformity of sensitivity, the great depth of the depicted space, the stereoscopic vision, the sensitivity to the polarization of radiation, and, finally, the amazing miniature of the compound eyes. Due to these properties, compound eyes are biological prototypes of many antenna arrays in engineering technologies [Solomatin, 2001].

- **3.2.2. Inherited phenomena of biological echolocation**

It is known that many organisms have an innate ability to echolocation based on directed rays of a wave nature, which is important for their life and survival [https://en.wikipedia.org/wiki/Animal_echolocation]. At the same time, due to the mechanisms of echolocation, for example, dolphins and bats can recognize not only the distance to the target but also the dimensions and shape of the objects they track, by analogy with how active digital antenna arrays (Smart Antennas) make it possible in technology (Fig. 3.2.1.1).

For example, the dolphin's receiving-radiating hydroacoustic system allows it to locate a pellet that has fallen into the water at a distance of 15 meters; distinguish between the material and dimensions of objects of the same shape, differing by a few percent; to distinguish, like a tomograph, the details of the internal structure and shape of objects in water or a layer of silt; detect edible fish at a distance of three kilometers and distinguishes it from those that do not go to food. There is evidence that dolphins can send images of objects to each other using their sonar systems [Prigg, 2015].

Sonar of dolphins uses the generation of ultrasonic vibrations by special membranes, which form a directed ultrasonic beam, the frequency and directivity pattern of which can change. It also uses many hydroacoustic receptors distributed at

a high density on the front side and a lower density over the surface of the entire body. These receptors "*form a multi-element broadband hydroacoustic receiving antenna with a circular pattern. This holographic reception subsystem provides illumination of the underwater environment, operating both in active and passive modes ... Dolphin has several hydroacoustic information systems that partially overlap each other and work in parallel*» [Leo, 2015]. Recall that mechanical and electromagnetic oscillations in organisms are interrelated since many biological tissues are piezoelectric.
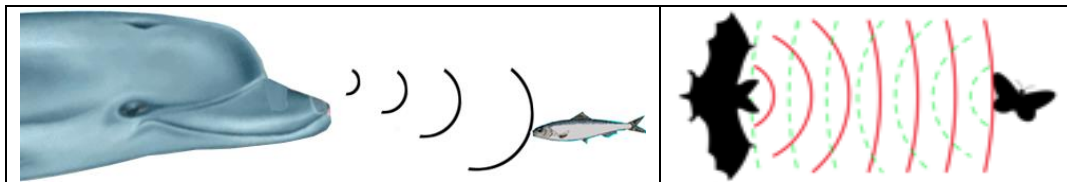
 Fig. 3.2.2.1. Examples of biological echolocation: echolocation in dolphins (left) and bats (from https://commons.wikimedia.org/wiki/File:Chiroptera_echolocation.svg, the picture is available under the Creative Commons CC0 License).

In wildlife, electrolocation is also widespread with the generation and reception of electric fields for solving by organisms many vital tasks of a search, evaluation, and communication nature. In active electrolocation, the animal senses its surrounding environment by generating electric fields and detecting distortions in these fields using electroreceptor organs [Albert, Crampton, 2006]. This electric field is generated using a specialized electric organ consisting of modified muscle or nerves. This field may be modulated so that its frequency and waveform are unique to the species and sometimes, the individual.

The perception of electric fields and their changes is usually carried out by many electroreceptors that are distributed throughout the body, forming bio-antenna arrays, the cumulative readings of which are processed by the body. For example, the platypus possesses receiving bio-antenna arrays having almost 40,000 electroreceptors arranged in a series of stripes along with the bill. These same abilities of electrolocation are used by organisms for electrical communication with other organisms. For example, weakly electric fish can also communicate by modulating the electrical waveform they generate, an ability known as electrocommunication [Hopkins, 1999]. They may use this for mate attraction and territorial displays.

In particular, electrolocation is used for jamming avoidance response, which is a behavior performed by some species of weakly electric fish. It occurs when two electric fish with wave discharges meet – if their discharge frequencies are very similar, each fish will shift its discharge frequency to increase the difference between the two fish's discharge frequencies. By doing this, both fish prevent jamming of their sense of electroreception [Bullock, Hamstra, Scheich, 1972]. Lists of literature and illustrations on electrolocation, electroreception, and electrical communications are available on the websites [https://en.wikipedia.org/wiki/Electroreception, https://en.wikipedia.org/wiki/Electrocommunication, https://en.wikipedia.org/wiki/Jamming_avoidance_response].

One of the biological examples of directed electromagnetic radiation is mitogenetic radiation, discovered in 1923 by A.G. Gurwitsch in experiments on cell proliferation of an onion [Beloussov, Voeikov, Martynyuk, 2007; Popp, 1992;

Voeikov, 2003; Volodyaev, Beloussov, 2015]. This radiation is associated with electromagnetic radiation in the ultraviolet range [Frank, 1982]. It is characterized by a high orientation, discovered by Gurvich himself and confirmed by the experiments of other authors [Inyushin, Chekurov, 1975].

One can note that the detection of objects and their geometric characteristics based on biological echolocation is an act of intellectual activity. Therefore, the phenomenon of biological echolocation is one the evidence in favor of the fact that the innate ability for intellectual activity in living organisms is based on inherited systems of bio-antenna arrays with their wave activity (smart bio-antennas, by analogy with Smart Antennas in technology). According to the author, the development of this topic of "system-antenna intelligence" will lead in the future to the understanding that bio-antenna arrays with their wave energy and self-organization mechanisms are not just transmitting and receiving devices, but they are the key participants of intellectual activity in the living.

We also note that researchers at Durham University (England) taught methods of biological echolocation to a group of blind and sighted people using a 10-week training program. Their study showed that the human body can learn the skills of biological click-based echolocation (the ability to learn click-based echolocation) regardless of age and degree of vision loss. The results of this work indicate the promise of teaching biological echolocation to people who are blind [Norman et al., 2021].

- 3.2.3. Inherited biophotonic crystals

This section presents information about the inherited sets of interconnected biophotonic crystals that form bio-antenna array systems.

Modern engineering technologies actively use so-called photonic crystals to control the spatial distribution of photon beams [Joannnopoulos et al., 2008; Hasan, Helleso, 2021; Krasnok et al., 2013]. The technologies of antennas and antenna arrays based on photonic crystals are being intensively developed [Zaitsev, 2011]. A photonic crystal is a periodic optical nanostructure that affects the motion of photons. Photonic crystals contain regularly repeating regions of high and low dielectric constant. Photons (behaving as waves) either propagate through this structure or not, depending on their wavelength. This gives rise to distinct optical phenomena, such as inhibition of spontaneous emission, high-reflecting omnidirectional mirrors, and low-loss-waveguiding. The periodicity of the photonic crystal structure must be around half the wavelength of the electromagnetic waves to be diffracted. One should note that, as known, living bodies possess inherited opportunities to manage photonic beams using physical principles of photonic crystals with their properties of photon gratings, etc. Many inherited biological phenomena of structural coloration and animal reflectors are built on this, including a beautiful coloring of butterfly wings, peacock feathers, etc. (see details and lists of references in [https://en.wikipedia.org/wiki/Photonic_crystal,

https://en.wikipedia.org/wiki/Animal_reflectors, https://en.wikipedia. org/wiki/Structural_coloration]).

Figs. 3.2.3.1 and 3.2.3.2 show some examples of inherited interrelated regular manifolds of biophotonic crystals forming biological analogies of technical antenna arrays. These examples give pieces of evidence that living bodies with their genetic system skillfully encode and inherit entire manifolds of bio-antenna arrays.

a)   b)   c)
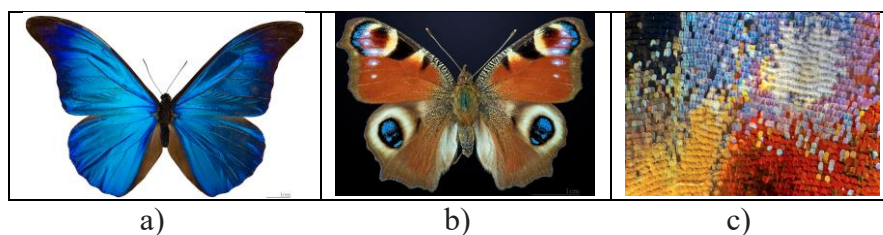
Fig. 3.2.3.1. Photonic crystals form heritable species patterns on butterfly wings, which allow differentiation between different species of butterflies.
a)   Rhetenor   Blue   Morpho   (from https://commons.wikimedia.org/wiki/File:Morpho_rhetenor_rhetenor_MHNT_dos.jpg, the image is available for distribution under the Creative Commons CC0 License)
b) European peacock (from https://commons.wikimedia.org/wiki/File:Paon-du-jour_MHNT_CUT_2013_3_14_Cahors_Dos.jpg, the image is available to share under the Creative Commons CC0 License);
c) regular sets of photonic crystal scales on a wing of a peacock butterfly (Aglais io) under the microscope (from https://ru.wikipedia.org/wiki/Чешуекрылые, the image is available to share under the Creative Commons CC0 License).

The amazing coloring of peacock feathers is due to the play of light on the photonic crystals in them [Blau, 2004]. The chameleon also changes the color of its body reversibly, using multiple photonic crystals on its surface and optical interference on them. This was recently established by studies by Swiss scientists who revealed the existence in the skin of chameleons of two layers of cells with highly ordered structures of small (~ 130 nm) photonic nanocrystals of the guanine, which serves as one of the nitrogenous bases in DNA [Teyssier et al., 2015]. Tension or relaxation in the system of these cells helps animals to quickly change color by changing the ability of the skin to reflect light.
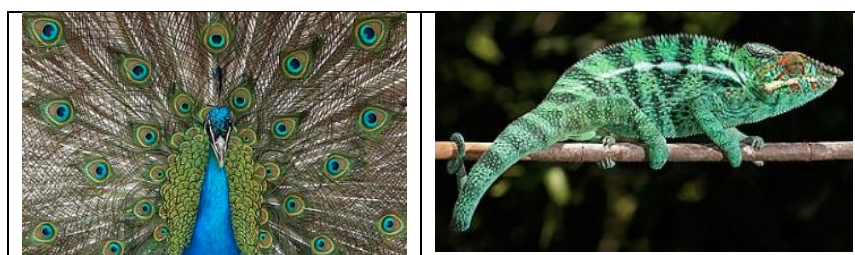
Fig. 3.2.3.2. Peacock feather coloring and body-color changes in chameleons are linked to ordered inherited arrays of biophotonic crystals (from https://en.wikipedia.org/wiki/Indian_peafowl   and https://en.wikipedia.org/wiki/Chameleon; these images are available to share under the Creative Commons Attribution 3.0 Unported license and the Creative Commons Attribution-Share Alike 4.0 International license.

Many animals in nature such as fish or beetles employ responsive photonic crystals, which form matrix structures, in their intelligent-like activities for camouflage, signaling, or baiting their prey [Hui, Ke-Qin, 2013; https://en.wikipedia.org/wiki/Photonic_crystal_sensor].
It is natural to assume that the genetic transfer of inherited properties of

photonic crystals in biological bodies is built on the that the molecular genetic structures themselves possess the properties of photonic crystals. One can remind here the Schrödinger's definition of chromosomes as aperiodic crystals [Schrödinger, 1944].

We believe that spatial characteristics of ensembles of genetic and other biological molecules, that form complex diffraction structures, play a managing role of photonic crystals in the problem of controlling photon beams that are generated and absorbed by these molecules (the range of photon frequencies in living bodies can be very wide, far beyond the optical range).

In our opinion, the inherited morphogenetic processes in living bodies are also determined to a large extent by biological photon beams, the course of which is not accidental, but is strictly organized by a system of spatial characteristics of ensembles of genetic and other biological molecules as photonic crystals. In the course of ontogeny, based on electromagnetic (photonic) interactions, new molecular materials are involved in a naturally growing biological body, which leads to the appropriate growth of the managing system of biophotonic crystals and the growth of numbers of photon beams. Of course, quantum-mechanic laws of resonances in molecular photonic interactions play an important role. Photonic crystals are related to the topic of nanoantenna arrays in two ways [Zaitsev, 2011; Herman, 1986; Shishkin, Shishkina, 2009].

1) They are used in optical nanoantenna and microwave technologies. Usually, a nanoantenna is understood as a miniature antenna, the dimensions of which do not exceed hundreds of microns, and one of the dimensions is 100 or fewer nanometers. Nanoantennas are also often referred to as nanodevices that allow the scattering of radiation in a given direction [Krasnok et al., 2013]. Photonic crystals and their lattices are such devices;

2) The location of many photonic crystals as a screen next to the nanoantenna can change its functional characteristics. In particular, the fluorescence of a single molecule that enters the nanoantenna gap can be increased by a factor of 10 [Krasnok et al., 2013].

In engineering technics, photonic crystals are composed of a periodic dielectric, Metallo-dielectric—or even superconductor microstructures or nanostructures. As it is known, active biological systems have extraordinarily high dielectric properties [Fröhlich, 1988]. For this reason, just dielectric photonic crystals, which have wide application in technics and are actively analyzed in the theory of photonic crystals and their applications in antenna arrays, are the most interesting for the theme of bio-antenna arrays.

One should add that the theme of nanoantennas, which are used in living nature for millions of years, is considered in modern science as very important: scientists believe that progress in technologies of corresponding nanoantenna production can lead to revolutions in computers (using photonics principles) and energetics (effective using of solar energy) [Krasnok et al., 2013; Zaitsev, 2011]. Nanoantennas are one of the elements needed to create quantum computers. The presented doctrine of the evolutionary role of bio-antenna arrays may be useful for understanding the mechanisms of photosynthesis in plant leaves.

- ### 3.2.4. Liquid biocrystals and heritable bio-antenna arrays

DNA and RNA are liquid crystal structures, like some other components of the living. The set of photonic crystals, particular cases of which are described in the previous section, contains a subclass of liquid crystal photonic crystals. Representatives of this subclass are among the most scientifically interesting and promising for applications of biophotonic structures.

Liquid crystal is a state of matter that has properties between those of conventional liquids and those of solid crystals [Sluckin, Dunmur, Stegemeyer, 2004]. For instance, a liquid crystal may flow like a liquid, but its molecules may be oriented in a crystal-like way. There are many different types of liquid-crystal phases, which can be distinguished by their different optical properties. Examples of liquid crystals can be found both in the natural world and in technological applications. Widespread liquid-crystal displays use liquid crystals. To date, tens of thousands of types of multicomponent liquid-crystal compounds have been synthesized for technical purposes around the world.

Due to the anisotropy of their structure, liquid crystals can scatter electromagnetic waves incident on them in selected directions. If a liquid crystal object has dimensions characteristic of nanoantenna arrays, then due to this anisotropic ability, it can serve as a nanoantenna array (as was above mentioned for nanoantennas in the previous section). Emission at a photonic bandgap created by the periodic dielectric structure of the liquid crystal gives a low-threshold high-output device with stable monochromatic emission [Kopp et al., 1998; Dolgaleva et al., 2008].

Lyotropic liquid-crystalline phases are abundant in living systems, the study of which is referred to as lipid polymorphism. Accordingly, lyotropic liquid crystals attract particular attention in the field of biomimetic chemistry. In particular, biological membranes and cell membranes are a form of liquid crystals. These liquid crystal membrane phases can also host important proteins such as receptors freely "floating" inside, or partly outside, the membrane. Many other biological structures exhibit liquid-crystal behavior. For instance, the concentrated protein solution that is extruded by a spider to generate silk is, in fact, a liquid crystal phase. DNA and many polypeptides, including actively-driven cytoskeletal filaments can also form liquid crystal phases [Wensink et al., 2012]. Together, these biological applications of liquid crystals form an important part of current academic research. The piezoelectric effect exists in liquid crystals; for this reason, interrelated electromagnetic and vibrational phenomena can coexist in them [Denisova, Scaldin, 2013].

As noted above, antenna arrays are capable of generating narrow and precision directional electromagnetic beams of multiply enhanced intensity. Getting in a targeted way on the piezoelectric areas in living tissues, such electromagnetic influences cause mechanical vibrations in the corresponding small (almost point) areas. Therefore the wave activity of bio-antenna arrays can lead to a very heterogeneous distribution of piezoelectric vibrations in cells and other tissue structures. These heterogeneous influences from one of the bio-antenna arrays on biological tissue can also lead to spatial-temporal reorganizing of other bio-antenna arrays in this tissue. Such interrelated wave influences of different bio-antenna arrays on each other, which reorganize their interconnected antenna systems, are participants of self-organization in living bodies.

Of particular interest for biological and applied research are liquid crystals called chiral phases or twisted nematics. For these crystals, the direction of the orientation of molecules in successive layers changes in a spiral (Fig. 3.2.4.1).
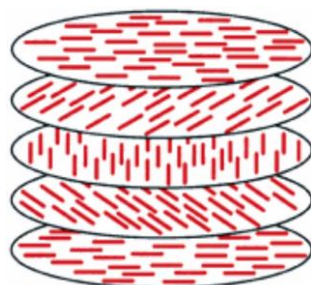
Fig. 3.2.4.1. Chiral nematic phase (from https://en.wikipedia.org/wiki/Liquid_crystal; the image is available to share under the Creative Commons Attribution-Share Alike 3.0 Unported license).

As a rule, chiral nematic crystals are obtained from compounds with pronounced anisotropy - the unequal properties in different directions. It is these properties that, as is known, DNA and RNA, which are naturally twisted into a double helix, possess. It can be said that the desire for such helical chiral packing is an "inherent" property of their double-stranded molecules.

Since their nitrogenous bases absorb ultraviolet, these chiral nematic crystals, when obtained in the laboratory, have a peculiar "color", which manifests itself in the form of an abnormally high optical activity (the ability to rotate the radiation polarization plane), which is tens and hundreds of times higher than the optical activity of single molecules [Yevdokimov et al., 2012]. This fact emphasizes the need to take into account the emergent properties of multi-element nanoantenna arrays and their wave activity, which are fundamentally different from the properties of a single nanoantenna.

The chiral twisting that occurs in chiral liquid-crystal phases also makes the system respond differently from right- and left-handed circularly polarized light. These materials can thus be used as polarization filters [Fujikake et al., 1998]. The theme of circularly polarized light from biological chiral liquid crystals is connected with the fundamental problem of biomolecular asymmetry by L.Pasteur [Flack, 2009]. Sets of helical chiral biomolecules can serve as helical antenna arrays, which radiate and absorb electromagnetic waves of the corresponding circular polarization. This provides the opportunity for helical chiral biomolecules to exchange radio waves of the corresponding circular polarization selectively with helical biomolecules of the same kind of chirality. In radio transmission technologies, circular polarisation is often used where the relative orientation of the transmitting and receiving antennas cannot be easily controlled, such as in animal tracking and spacecraft communications (that is, for example, a spacecraft rotation does not influence the communication). In other words, regarding these helical antenna arrays, the factor of chirality (left or right polarization) is very important for communication. We add that the directional properties of a helical axial radiation antenna can be determined by considering the spiral as a linear antenna array consisting of some emitters - turns [Voskresensky et al., 2006, p.287]. The author believes that the principle of the chiral stereochemical organization of biomolecules in living nature is deeply related to the informational principle of communication among biomolecules based on bio-antenna arrays

working with electromagnetic waves of appropriate circular polarization. Helices are termed long ago as «*curves of life*» due to the multiple implementations of inherited helical structures and processes in living bodies on various lines and levels of biological evolution [Cook, 1914; Petoukhov, Svirin, Khazina, 2015]. For example in the human body, helical structures are genetically inherited from generation to generation in muscles, heart, vessels, bones, tendons, ligaments, nerves, organs of hearing (cochlea ear), etc.

An analog of a spiral antenna in a form of left-handed helices was recently discovered by Swedish scientists in the tail of a spermatozoon. These authors speculate that these helical structures in particular can «play a role in controlling the swimming direction of spermatozoa» that plays the role of antennas for communication with the environment [Zabeo et al., *Scientific Reports*, 2018].

The ability of biological molecules to such spontaneous formation of ordered ensembles is important not only for the life and development of organisms but also for the technical nano-design of new molecular structures and their ensembles to create new drugs, sensors, nano-robots, etc. Researchers note the chemical diversity of biological "building blocks" (amino acids, lipids, nucleotides) for such nano-constructions, as well as their tendency to the spontaneous formation of complex spatial structures [Yevdokimov et al., 2012].

For example, it has been observed that concentrated solutions of short DNA oligomers develop liquid crystal ordering as the result of a hierarchically structured supramolecular self-assembly; this finding suggests a novel scenario for the abiotic origin of nucleic acids [Fraccia et al., 2015]. One can mention that phenomena of self-organization of nanostructures are intensively studied in modern science [Feltz B. et al., 2006]. From the point of view of convenience for nano-assembly technologies, nucleic acids have the best properties [Yevdokimov et al., 2012].

Nanoantennas based on DNA are already used in scientific technologies: scientists at the University of Montreal in Canada have created glowing nanoantennas from DNA molecules to track the relationships within proteins. These nanoantennas are capable of fluorescence and can absorb radiation at one wavelength and emit light at a different frequency depending on the molecular environment [Harroun et al., 2022].

The structural properties of liquid crystals combine probabilistic and deterministic characteristics. The liquid crystal in the simplest case is a structure consisting of ordered molecular layers, which still retain some diffusion degrees of freedom characteristic of the behavior of molecules in a liquid solution. There is a well-known comparison of liquid crystals with a stream of logs floated down a river: in general, they are all lined up in the same direction, downstream, although each log floats on its own [Yevdokimov, 2005]. Thus, in the properties of liquid crystals, the "probability-determinism" dualism is represented at the molecular level, which is characteristic of biological phenomena of various levels and considered in Gestal genetics and Gestalt biology [Petoukhov, 2021a]. We also note that the chemical composition of liquid crystals can be very different from the external similarity of their integral configuration.

4. Regarding regeneration phenomena, genetics, and antenna arrays

The cells of a multicellular organism must exchange information for their coordinated behavior in the processes of ontogenesis and current life activity. This implies the presence of a system of long-distance information links between many

cells of the body. Violation of these connections is fraught with oncology, morphological deformities, and other negative consequences. The activity of bio-antenna arrays that emit and receive electromagnetic waves can be one of the types of long-range information links between cells and other structures of the body. At the same time, in biological piezoelectric media, electromagnetic waves generate mechanical vibrations and waves.

It has already been noted above that many living organisms have an innate ability for electrolocation and electrical communication. It is natural to believe that these abilities for remote wave electrical signal communication, inherited from generation to generation, did not arise from scratch, but are a continuation of the forms of electromagnetic wave communication between elements within the body itself. These electromagnetic forms exist alongside well-known biochemical communications using the exchange of molecular elements, as well as communications based on the action of mechanical forces. The neurons of the nervous system, with their action potentials, are a well-known example of remote signaling based on bioelectricity. Modern data from some authors suggest that the bioelectrical connection between cells of other types that are not neurons is also used as a means of remote communication (see, for example, [Levin, Martyniuk, 2018]).

In connection with the topic of long-range operational communication between the elements of the body, let us recall the above-mentioned remarkable emergent properties of antenna arrays, which are ensured precisely by the coordinated combination of many individual antennas into a single system and which are used in bio-antenna arrays inside the body:

-1) the possibility of generating and receiving precision directed beams (including narrow beams for point zones) with multiple increases in the level of radiated and received power;

-2) the possibility of emission and reception of many such beams at once, having different frequencies and other characteristics and independent of each other;

- 3) Antenna arrays are a unique tool for providing communication noise-immunity and extracting a weak signal from a strong noise;

- 4) ensuring the noise immunity of information messages with the possibility of adapting to the interference environment.

For the design and calculation of digital antenna array systems in technology, their tensor-matrix theory was developed [Slyusar, 1999], which, in particular, allows you to create new approaches to artificial intelligence systems [Slyusar, 2021]. Its algebraic formalisms turned out to be related to matrix-tensor genetics developed by the author of this article [Petoukhov, 2008, 2019-2021; Petoukhov, He, 2010]. This gives an additional reason to think that the intellectual properties of living organisms and their subsystems can be based on the energy-information activity of bio-antenna arrays systems. As noted above, the functioning of bio-antenna arrays in physiological systems, for example, in echolocation and faceted organs of vision, is directly related to the performance of intellectual functions of searching and evaluating objects of the external world.

The problem of inherited intellectual abilities has acquired particular relevance in connection with the creation of artificial intelligence systems. In this case, the following point of view is known: «*In fact, intelligence—a purposeful response to available information, often anticipating the future—is not restricted to the minds of some privileged species. It is distributed throughout biology, at many different spatial and temporal scales. There are not just intelligent people, mammals, birds, and cephalopods. Intelligent, purposeful problem-solving behavior can be found in parts*

of all living things: single cells and tissues, individual neurons and networks of neurons, viruses, ribosomes, and RNA fragments, down to motor proteins and molecular networks… Modern biology faces a fundamental knowledge gap when trying to explain meaningful, intelligent behavior. How can a system composed of cells and electrical signals generate a well-adapted body with behavior and mental states? If cells are not intelligent, how can intelligent behavior emerge from a distributed system composed of them? This fundamental mystery permeates biology. All biological phenomena are, in a sense, "group decisions" because organisms are made of individual parts—organs, tissues, cells, organelles, molecules. What properties of living systems enable components to work together toward higher-level goals?" [Yuste, Levin, 2021]. The authors of the cited article argue that the architecture of modular systems underlies evolutionary and organismal intelligence.

They emphasize the basic meaning of the following evolutionary principles represented in biological bodies:

- 1) the principle of modularity;

- 2) the principle of a hierarchy of modules: "*lower-level modules combine to form increasingly sophisticated higher-levels modules, which then become new building blocks for even higher-level modules, and so on. Similarly, the local metabolic and signaling goals of the cells integrate toward a morphogenetic outcome of building and repairing complex organs. Thus, increasingly sophisticated intelligence emerges from hierarchies of modules*" [ibid].

But these principles are actively used in the engineering construction of modular digital antenna arrays (smart antenna) where lower-level antenna arrays of modular type are combined to form increasingly sophisticated higher-level modules, which then become new building blocks for even higher-level modules, and so on (systems of antenna arrays-subarrays-subsubarrays-...). It is one of the additional arguments in favor of a basic meaning of bio-antenna arrays for the development and providing of biological intelligence.

Cells are one of the important types of biological modules from which a living organism is built. Many of the key elements of a cell, such as its DNA, membranes, many polypeptides, and cytoskeleton, are liquid crystals [Gupta et al., 2015; Schakenraad et al., 2020]. These crystals, as mentioned above, can serve as liquid crystal nanoantenna arrays. At the same time, they can participate in intellectual activity at the cellular level. We note in passing that the cytoskeleton of neurons has long been considered by some authors as a computing environment when nerve cells perform their tasks [Lieberman et al., 2008]. The activity of transceiver liquid crystal bio-antenna arrays can be considered a special chapter of bioelectric physiology. They have connections with endogenous bioelectric fields and have been shown to regulate many patterning, morphological, and regenerative processes [McLaughlin, Levin, 2018; Levin, Martyniuk, 2018].

It is natural to believe that the electromagnetic wave activity of liquid crystal and other nanoantenna arrays of cells is involved, among other things, in the distribution of rest potentials on cell membranes. This applies, in particular, to the cells of the initial stages of the formation of a multicellular organism. In turn, an artificial change in electrical potentials on cellular liquid crystal membranes under the influence of external factors (for example, under the influence of ionophores) can cause rearrangements in the organism's system of bio-antenna arrays and their functioning.

The location in the cell of DNA molecules and cytoskeleton elements involved in the activity of transmitting and receiving bio-nanoantenna arrays is characterized

by a certain asymmetry and polarity, which may be involved in the phenomenon of the polarity of the distribution of potentials on the cell membrane. We emphasize this in connection with the fact that the polarity of the distribution of potentials on cell membranes is important for morphogenetic processes and the regeneration of organs and tissues. This is shown by the impressive results of the experimental works of M. Levin and his colleagues at Tufts University, USA [https://ase.tufts.edu/biology/labs/levin/publications/, https://www.youtube.com/watch?v=XheAMrS8Q1c].

These works were carried out on flatworms - planarians, which have a head, a true brain, and many other organs, including a tail. Planarians are champions in organ and tissue regeneration and, in this regard, have been studied in biology, including bioelectric physiology, for over 100 years. if you cut its body into pieces - for example, into 200 pieces - every piece will rebuild exactly what's needed to make a perfect little worm. This is a system where every single piece knows exactly what a correct planarian looks like and builds the right organs in the right places and then stops. In the works of Levin and his colleagues, it was shown that the determination of the correct position of the organ in the body of the worm occurs due to bioelectric potentials and is controlled by the distribution of membrane potentials in not yet differentiated cells. Differences between the cells of the head and tail appear in the first three hours after amputation. In these works, it was shown that an artificial change (with the help of ionophores without application of external electrical influence) of the typical distribution of the membrane potential on an amputated fragment of the worm's body leads to the formation of planarians with two heads and sometimes an unusual body shape [Durant et al., 2019].

It is especially remarkable that if both heads are cut off from the resulting two-headed worm, then a two-headed worm is again formed from the remaining middle fragment. And this procedure can be repeated many times, each time receiving the regeneration of a two-headed worm. This means that the memory of the correct structure of the body, which should be formed after regeneration, turns out to be radically changed, although the genome of this organism did not change and remained the same. Therefore, the memory that tells the worm about how many heads it should have is contained not in the genome at all!

These experimental facts have led Levin to the important idea that emergent phenomena of an ensemble of cells are key participants of morphological and some other processes. More precisely, the association of cells into a multicellular ensemble leads to the manifestation of emergent properties in the emerging supracellular system: such multicellular ensembles can determine the type of morphological patterns formed, largely independently of the information in DNA, which is essential for coding of proteins. This new point of view, justified by Levin, is very different from the widespread idea that the information sequences of DNA and RNA determine everything in a developing organism. It is quite possible that each higher level of combining of cells and supracellular structures into ensembles exhibits its emergent properties, that is, the development and behavior of complex multicellular organisms are determined by a multilevel system of emergent properties.

Taking into account the mentioned experimental results, Levin puts forward the concept that «the *electrical blueprints orchestrate life*» [Levin, 2020]. More precisely, he believes that all cells in our body communicate with each other using electrical signals. Corresponding electrical networks of cells (much like networks on the brain) are formed, which process information including pattern memories in the same way that brains hold other kinds of memory and learning. Besides this, Levin writes that

these electrical signals have a bioelectrical code to control growth and form. A feature article on the bioelectric code highlights the importance of cracking it: "*We review emerging progress in reading and re-writing anatomical information encoded in bioelectrical states… Cracking the bioelectric code will enable much-improved control over biological patterning, advancing basic evolutionary developmental biology as well as enabling numerous applications in regenerative medicine and synthetic bioengineering*" [Levin, Martyniuk, 2018].

The idea that cell systems combined into an ensemble have emergent properties led Levin to fruitful experiments on combining genetically unchanged cells into an ensemble. These experiments showed that from the union of such cells, each of which has its evolutionary history, organisms that have never existed before can arise. For example, Lewin showed that the combination of cells from the skin of a frog into a single ensemble leads to the appearance of a tiny body of a completely new design. Such bodies, which are biological robots called xenobots, can move, navigate a labyrinth, explore the environment, feed and heal themselves, and exhibit emergent group behavior, although they do not have a nervous system, do not have a brain, and are simply collections of skin cells, who can explore the environment and move around. These xenobots can live 10-14 days. A list of freely available publications by Levin and his co-authors on topical issues of regenerative medicine and the creation of "living machines" - xenobots - is given on the website https://ase.tufts.edu/biology/labs/levin/publications/. An overview video of Levin's interview is available on YouTube [Levin, 2020].

Our doctrine of energy-informational evolution based on bio-antenna arrays is also based on the idea of the emergence of system properties: the functional capabilities of bio-antenna arrays that combine many antenna elements radically exceed the capabilities of individual antenna elements. But this doctrine is broader than Lewin's concept that "the electrical blueprints orchestrate life" and differs significantly from it. These differences are characterized by the following main statements of our doctrine, which may be, in particular, useful for understanding the results of the experiments of Levin and his colleagues:

1. In the biological connection between the parts of each bio-body, an important role is played by electromagnetic waves of bio-antenna arrays (in addition to bioelectric communication based on distributed electrical potentials and the exchange of electrical signals). Thus, the participants in this connection are also the magnetic components of these waves and not just electrical potentials;
2. Electromagnetic waves of bio-antenna arrays cause mechanical vibrations in a variety of piezoelectric biological media; these vibrations can generate a whole class of additional mechanical phenomena in bio-bodies, sometimes striking in their unusualness and unexpectedness, as noted above;
3. The emergent property of bio-antenna arrays to operate with narrowly directed beams of electromagnetic waves (including operating simultaneously with many independent beams having a different frequency, phase, polarization, and other characteristics) provides targeted and selective connections between many different elements of the body, including remote from each other;
4. The emergent property of phased antenna arrays to change the direction and intensity of rays of produced and received wave radiation due to a change in the phase relationships in the operation of their individual antennas (without moving the antennas themselves) gives a new approach to the theme of cyclic processes in biological bodies: corresponding changes in the phase ratios of

the elements of bio-antenna arrays make it possible to rebuild the spatial-temporal characteristics of wave energy rays, cyclically redirecting and redistributing internal energy flows in space and time to provide cyclic activations and deactivations of biological components;

5. The types of polarization of electromagnetic waves of bio-antenna arrays must be taken into account when considering the relationships between the elements of the bio-body since they are associated with the problems of biological dissymmetry and molecular chirality, which have been considered in science since the time of L. Pasteur (many organisms are known to have polarization vision and distinguish between types of polarization light photons);

6. The unique ability of antenna arrays to provide noise-resistant multi-channel operation with the extraction of weak signals against the background of strong noise allows us to rethink the phenomenal ability of organisms to work with weak information signals against the background of strong noise in many parallel channels with providing information noise immunity. According to Mendel's law of independent inheritance of traits, information from the level of DNA molecules dictates the macrostructure of living bodies through many independent channels, despite strong noises. For example, hair, eye, and skin colors are inherited independently of each other. Accordingly, each organism is a machine of multichannel noise-immunity encoding;

7. Electromagnetic waves from bio-nanoantenna arrays are photon fluxes, which in general are the subject of quantum mechanics and quantum informatics (in contrast to the problem of the distribution of electrical potentials on surfaces);

8. Memory and intellectual abilities are connected with systems of bio-antenna arrays and their wave coordinated activity;

9. Electromagnetic waves of bio-antenna arrays are involved in the operational transfer and redistribution of energy between the elements of the body.

Concerning point No. 9 about the role of bio-antenna arrays in energy flows in bio-bodies, the following should be added. The idea of the organizing role of coordinated energy flows inside the body exists since ancient times. It is associated with Ancient Chinese ideas about a certain special energy "qi" (or "chi"), on the characteristics of the circulation of which human health and illness depend and which determines the existence of energy pathways in the body, called acupuncture meridians. By the impact of acupuncture needles on these meridians, these energy flows can be tested and corrected. It cannot be ruled out that this mysterious energy "qi" is partially or completely precisely the energy of a multitude of coordinated electromagnetic and other wave rays from bio-antenna arrays. At the same time, the existence of oriented acupuncture meridians can be considered as one of the manifestations of the coordinated wave activity of bio-antenna array systems. As far as the author knows, in biology and biophysics, the possible biological significance of a self-organizing dynamic "web" (or openwork plexus) of narrowly directed rays of electromagnetic and other wave entities from bio-antenna array systems has never been considered; in this lace of beams and energy flows, there are interrelations and patterns associated with the principles of quantum mechanics and quantum informatics.

The algebraic analogies between the matrix-tensor representations of the universal rules of the stochastic organization of genomic DNAs (see above Section 2 with Figs. 2.1, 2.5) and the tensor-matrix theory of digital antenna arrays, also based on the

Hadamard product for matrices, described at the beginning of the article, additionally lead to the following new thoughts:

- Stochastic organization of information sequences of genomic DNAs is a special case of biological self-organization based on the wave activity of bio-antenna arrays, examples of which are presented at all levels of the body;
- The genetic code itself is one of the offspring of wave activity and self-organization of bio-antenna arrays, and this code is connected with other inherited physiological offsprings of bio-antenna arrays in the organism. The secret of the structural organization and origin of the genetic code, as well as the origin of organisms, must be sought not in the random combination of the molecular elements of the gene code, but in the emergent properties of self-organizing systems of bio-antenna arrays with their wave energy activity.

Accordingly, it is not genes that are the dictators of all life activity, since they themselves are built into the information-energy coherences of bio-antenna arrays and are produced by them. Dialects of the genetic codes arise in the course of the evolution of bio-bodies, when new living conditions appear and, if necessary, the dynamic systems of bio-antenna arrays associated with quantum mechanics are corrected. The genomes themselves and the genetic system are an integral part of the wave activity of ensembles of bio-antenna arrays and can be considered biological smart-antennas.

Previously, the author liked the well-known short definition of life: "*Life is a partnership between genes and mathematics*" [Stewart, 1999]. But in the light of the above facts, the author proposes a new short definition: "Life is a partnership of organisms with bio-antenna arrays and their wave energy". Of course, the role of mathematics in revealing the content of this definition, which is implicitly related to the algebraic theories of smart antennas and resonances, quantum mechanics, and quantum informatics, is exceptionally great.

5. Quantum mechanical aspects of the doctrine of evolution based on bio-antenna arrays

This section describes the theme of the affinity between the presented doctrine of bio-antenna evolution and the formalisms of quantum informatics and quantum mechanics, which are naturally used to model the features of the stochastic organization of genomic DNAs. Briefly speaking, the doctrine links together quantum informatics and antenna array theory based on genetic and physiological phenomena that testify to the expediency of considering such a connection.

Many authors have supposed that living organisms use principles of quantum informatics (Abbott, Davies, Pati, 2008; Altaisky, Filatov, 2001; Fimmel et al, 2019; Hu Z.B., Petoukhov, Petukhova, 2017a,b, 2018; Igamberdiev, 1993, 2004, 2007, 2008; Igamberdiev, Shklovskiy-Kordi, 2016, 2017; Josephson, 2018; Matsuno, 1999, 2003; Matsuno, Paton, 2000; Mikheenko, 2018; Patel, 2001a,b,c; Penrose,1996, 2019; Petoukhov, 2016, 2018a,b, 2019a,b). These principles include a principle of quantum entanglement, which has the key importance for the entire quantum informatics. The classic book [Nielsen, Chuang, 2010, p. xxiii] emphasizes: "*entanglement is a key element in effects such as quantum teleportation, fast quantum algorithms, and quantum error-correction. It is, in short, a resource of great utility in quantum computation and quantum information. There is a thriving research community currently fleshing out the notion of entanglement as a new type of physical resource,*

finding principles which govern its manipulation and utilization".

Usually, in speeches about quantum entanglements, researchers focus their attention on the entanglement of atoms and other elementary particles or the entanglement of spins. But in this section, the author draws attention to a question about quantum entanglement (or quantum-like entanglement) in quite other objects: stochastic information sequences of genomic DNAs.

Let's start with the fact that shown at the beginning of the article in Fig. 1.1 matrix representations of DNA-alphabets of 4 nucleotides, 16 duplets, 64 triplets, and, in general, 4^n n-plets $[C, A; T, G]^{\wedge}(n)$ form a single family of matrices based on the tensor product. The tensor product gives a way of putting separate vector spaces together to form larger vector spaces and it is one of the basic instruments in quantum informatics: "*This construction is crucial to understanding the quantum mechanics of multiparticle systems*" [Nielsen, Chuang, 2010, p. 71]. Thus, DNA informatics through the tensor interrelations in the system of DNA alphabets is connected with the formalisms of quantum informatics already at the level of the DNA alphabets.

Below it is presented that the quantitative characteristics of the stochastic organization of genomic DNAs (see examples in Fig. 2.1-2.9) show its connection with quantum informatics and the notion of "qubits", and, therefore, also the connection of this evolutionary doctrine with quantum informatics. In short, this doctrine, which includes the topic of nano-antenna arrays, includes also elements of quantum informatics connected with qubits, tensor products, Hilbert spaces, etc. As far as we know, some described quantitative relationships related to qubits are absent in the engineering systems of antenna arrays, and therefore they are a distinctive feature of this biological doctrine (correspondingly bio-antenna arrays should be considered as a very particular case of all possible set of antenna arrays).

Besides this, the above-noted operation of the Hadamard product of matrices, which made it possible to algebraically express the phenomenologic relationship of genomic probability matrices (Fig. 2.1, 2.5), is also used in quantum informatics; this fact allows us to take a fresh look at the stochastic organization of genomic DNAs and this evolutionary doctrine in general from a quantum point of view. Let's explain this in more detail.

- **5.1. DNA alphabets, 2n-qubit systems, and quantum entanglement**

In this section, we will rely on the terminology of the classic book [Nielsen, Chuang, 2010] and use the generally accepted Dirac notation:
- $|\psi>$ means a vector, which is known also as a ket-vector;
- $<\psi|$ means a vector, which is dual to $|\psi>$ and known as a bra-vector;
- $<\varphi|\psi>$ means scalar (or inner) product between the vectors $<\varphi|$ and $|\psi>$;
- $|\varphi> \otimes |\psi>$ means the tensor product of $|\varphi>$ and $|\psi$.

In quantum informatics, those vector spaces H are considered, which are equipped with the scalar (or inner) product (so-called Hilbert spaces). Let H_1 and H_2 be quantum mechanical state spaces, that is, finite-dimensional Hilbert spaces with orthonormal basis states $|\alpha_i>$ and $|\beta_j>$, where i = 1, …, n and j = 1, …, m. By a postulate of quantum mechanics, the state space of the composite system is given by the tensor product $H_1 \otimes H_2$ with basis states $\{|\alpha_i> \otimes |\beta_j>\}$, or in more compact notation $\{|\alpha_i\beta_j>\}$. «*The state space of a composite physical system is the tensor product of the state spaces of the component physical systems*» [Nielsen, Chuang, 2010, p. 102]. If a quantum state can be represented as a vector of a Hilbert space, such a state is called a

pure quantum state. If a pure state $|\psi> \in H_1 \otimes H_2$ can be written in the form $|\psi> = |\psi_1>$ $\otimes |\psi_2>$, where $|\psi_i>$ is a pure state of the i-th subsystem, it is said to be separable. Otherwise, it is called entangled or non-separable [Nielsen, Chuang, 2010, p. 96].

As it is known, a quantum bit (or qubit) is a unit of quantum information. For two-level quantum systems used as qubits, the state $|0>$ is identified with the vector [1, 0], and the state $|1>$ with the orthogonal vector [0, 1]. Two possible states for a qubit are the states $|0>$ and $|1>$, which correspond to the states of 0 and 1 for a classical bit. The difference between bits and qubits is that a qubit can be in a state other than $|0>$ or $|1>$. It is possible to form linear combinations of states, often called superpositions (5.1.1):

$$|\psi> \ = \ \alpha|0> + \beta|1>, \qquad\qquad (5.1.1)$$

The symbol $|\psi>$ means a state of a qubit. The numbers α and β can be complex numbers but in our case, it is enough to think of them as real numbers. Put another way, the state of a qubit is a vector in a two-dimensional vector space. The standard notation for states in quantum mechanics is the Dirac notation "$| >$". The special states $|0>$ and $|1>$ are known as computational basis states and form an orthonormal basis for this vector space [Nielsen, Chuang, 2010, p. 13]. As known, we cannot examine a qubit to determine its quantum state, that is, the values of α and β. Instead, quantum mechanics tells us that we can only acquire much more restricted information about the quantum state. When we measure a qubit we get either the result 0, with probability $|\alpha|^2$, or the result 1, with probability $|\beta|^2$. Naturally, $|\alpha|^2 + |\beta|^2 = 1$, since the probabilities must sum to one. Geometrically, we can interpret this as the condition that the qubit's state is normalized to length 1. Values α and β are called amplitudes of probabilities. Thus, in general, a qubit's state is a unit vector in a two-dimensional complex vector space. Let us emphasize again that when a qubit is measured, it only ever gives "0" or "1" as the measurement result – probabilistically.

In the more general case, a system of "n" qubits is considered in quantum informatics. The computational basis states of this system are written in the form $|x_1 x_2 ... x_n>$; a quantum state of such a system is specified by 2^n amplitudes [Nielsen, Chuang, 2010, p. 17]. In our model approach, we in general interpret each of the considered n-plet texts of genomic DNAs as a multi-qubit quantum system.

In technical devices of quantum informatics, a qubit can be represented in many ways based on different pairs of binary-oppositional indicators: for example, by two electronic levels of an atom; by two kinds of polarization of a single photon (vertical polarization and horizontal polarization), etc.

In our model approach for genetic informatics, we represent qubits based on different pairs of binary-oppositional indicators of adenine A, guanine G, cytosine C, and thymine T, which were shown above in Fig. 1. As we noted, each of these DNA bases can be uniquely defined by two kinds of mentioned binary-oppositional indicators (Fig. 1.1). More precisely, to characterize each of the DNA letters C, A, T, G we will use the binary-oppositional indicators "amino-or-keto" (C=A=0, T=G=1) and the binary-oppositional indicators "pyrimidine-or-purine" (C=T=0, A=G=1) like as in Fig. 1.1. Based on each of these pairs of binary-oppositional indicators, two options of qubits can be considered under a model representation of stochastic genomic DNAs sequences as quantum systems (those qubits, which are introduced in genetic informatics based on binary-oppositional indicators of genetic molecules, can be conditionally called «genetic qubits» or briefly «g-qubits»).

Let us introduce, firstly, the notion of a genetic qubit as a two-level quantum system, which represents a considered genomic DNA based on the indicators «amino-or-keto»: in this quantum system one level corresponds to the indicator «amino» and the second level – to the oppositional indicator «keto». In other words, such genetic qubit is represented by these oppositional indicators, and the state of such qubit is a vector in its appropriate two-dimensional Hilbert space H_1. One can assume that the state $|0>$ corresponds to the state «amino», and the state $|1>$ - to the state «keto» (we mark these states by red to emphasize their relations to the red binary numeration of rows of matrices in Figs. 1.1-1.4). By analogy with the expression (5.1.1), a state of such genetic qubit can be shown by the expression (5.1.2), where α_0 and α_1 are amplitudes of probabilities of these computational basis states "amino" and "keto":

$$|\psi_1> = \alpha_0 |0> + \alpha_1 |1>, \qquad \alpha_0^2 + \alpha_1^2 = 1 \qquad (5.1.2)$$

The qubit (5.1.2) corresponds to a pure state of a quantum system in a form of a DNA stochastic sequence of amino and keto molecules.

Secondly, let us introduce the notion of another genetic qubit as a two-level quantum system, which represents a considered genomic DNA based on the indicators «pyrimidine-or-purine»: in this quantum system, one level corresponds to the indicator «pyrimidine» and the second level – to the indicator «purine». In other words, this genetic qubit is represented by these two indicators, and the state of such qubit is a vector in its appropriate 2-dimensional Hilbert space H_2. One can assume that the state $|0>$ corresponds to the state «pyrimidine», and the state $|1>$ - to the state «purine» (we mark these states by blue to emphasize their relations to the blue binary numeration of columns of matrices in Figs. 1.1-1.4). By analogy with the expression (5.1.1), a state of such genetic qubit can be expressed by the expression (5.1.3), where β_0 and β_1 are amplitudes of probabilities of these computational basis states:

$$|\psi_2> = \beta_0 |0> + \beta_1 |1>, \qquad \beta_0^2 + \beta_1^2 = 1 \qquad (5.1.3)$$

The qubit (5.1.3) corresponds to a pure state of a quantum system in a form of a sequence, which consists of pyrimidines and purines.

So we have two different 2-dimensional Hilbert spaces H_1 and H_2, to which pure states of genetic qubits (5.1.2) and (5.1.3) belong correspondingly. In our genetic case, the tensor product of the two-dimensional Hilbert space gives one 4-dimensional Hilbert space $H_{12} = H_1 \otimes H_2$, whose vectors correspond to appropriate 2-qubit systems. Its 4 computational basis states are expressed by the tensor product of the computational basis states of its subspaces H_1 and H_2 and have the following forms, corresponding to 4 nitrogenous bases C, A, T, and G:

- $|00>$ corresponds to C defined by the pair of indicators "amino and pyrimidine";
- $|01>$ corresponds to A defined by the pair of indicators "amino and purine";
- $|10>$ corresponds to T defined by the pair of indicators "keto and pyrimidine";
- $|11>$ corresponds to G defined by the pair of indicators "keto and purine".

These 4 computational basis states $|00>$, $|01>$, $|10>$, $|11>$ symbolize 4 orthonormal basis vectors [1, 0, 0, 0], [0, 1, 0, 0], [0, 0, 1, 0], [0, 0, 0, 1]. The computational basis states can be also denoted as $|C>$, $|A>$, $|T>$, $|G>$, and correspondingly their amplitudes of probabilities can be denoted as γ_C, γ_A, γ_T, γ_G in a general case.

In a general case, corresponding 2-qubit systems are presented by the expression (5.1.4):

$$|\psi_{12}> = \gamma_{00}|00> + \gamma_{01}|01> + \gamma_{10}|10> + \gamma_{11}|11> \qquad (5.1.4)$$

where the normalization condition should be fulfilled:

$$(\gamma_{00})^2 + (\gamma_{01})^2 + (\gamma_{10})^2 + (\gamma_{11})^2 = 1 \qquad (5.1.5)$$

There are two following options exist for the interrelation between amplitudes of probabilities γ_{00}, γ_{01}, γ_{10}, γ_{11} of the 2-qubit state $|\psi_{12}>$ and amplitudes of probabilities α_0, α_1, β_0, β_1 of the qubits states $|\psi_1>$ and $|\psi_2>$.

The first option is if these amplitudes are interrelated by the equalities (5.1.6):

$$\gamma_{00} = \alpha_0\beta_0, \quad \gamma_{01} = \alpha_0\beta_1, \quad \gamma_{10} = \alpha_1\beta_0, \quad \gamma_{11} = \alpha_1\beta_1 \qquad (5.1.6)$$

It is realized in the case, if the state $|\psi_{12}>$ can be expressed by the tensor product of the states $|\psi_1>$ and $|\psi_2>$:

$$|\psi_{12}> = |\psi_1> \otimes |\psi_2> = (\alpha_0|0> + \alpha_1|1>) \otimes (\beta_0|0> + \beta_1|1>) =$$

$$\alpha_0\beta_0|00> + \alpha_0\beta_1|01> + \alpha_1\beta_0|10> + \alpha_1\beta_1|11> \qquad (5.1.7)$$

In quantum informatics, such state $|\psi_{12}>$ is called a pure separable state. The sign of the tensor product here indicates that these subsystems are completely independent of each other.

The second option is if the state $|\psi_{12}>$ cannot be expressed by the tensor product of the states $|\psi_1>$ and $|\psi_2>$. In this case the state $|\psi_{12}>$ is called non-separable or entangled, and you have inequalities such as in (5.1.8):

$$|\psi_{12}> \neq |\psi_1> \otimes |\psi_2>, \ \gamma_{00} \neq \alpha_0\beta_0, \ \gamma_{01} \neq \alpha_0\beta_1, \ \gamma_{10} \neq \alpha_1\beta_0, \ \gamma_{11} \neq \alpha_1\beta_1 \qquad (5.1.8)$$

Let's study which of these two options is realized by Nature, for example, in the DNA of human chromosome № 1. In this DNA, the percentage α_0^2 of amino

molecules (C and A) is equal to 0.499500, and the percentage α_1^2 of keto molecules (T and G) is equal to 0.500500 (rounding to the sixth decimal place). In other words, $\alpha_0^2 \approx \alpha_1^2$ by Chargaff's second parity rule, which states that %C ≈ %G and %A ≈ %T in enough long single-stranded DNAs (correspondingly you have %C+%A ≈ %T+%G for long single-stranded genomic DNAs).

In the considered DNA, the percentage β_0^2 of pyrimidines (C and T) is equal to 0.500255, and the percentage β_1^2 of purines (A and G) is equal to 0.499745 (rounding to the sixth decimal place). In other words, $\beta_0^2 \approx \beta_1^2$ by Chargaff's second parity rule as well. Using these phenomenologic data, you have the following amplitudes of probabilities for computational basis states |00>, |01>, |10>, |11> in a supposed case of the pure separable states (5.1.7):

$$\alpha_0\beta_0 = 0.499500^{0.5} * 0.500255^{0.5} = 0.499877,$$
$$\alpha_0\beta_1 = 0.499500^{0.5} * 0.499745^{0.5} = 0.499622,$$
$$\alpha_1\beta_0 = 0.500500^{0.5} * 0.500255^{0.5} = 0.500377,$$
$$\alpha_1\beta_1 = 0.500500^{0.5} * 0.499745^{0.5} = 0.500122. \qquad (5.1.9)$$

Resuming, in the supposed case of pure separable states (5.1.7) of the considered chromosomal DNA, you should have approximate equalities of all amplitudes of probabilities:

$$\alpha_0\beta_0 \approx \alpha_0\beta_1 \approx \alpha_1\beta_0 \approx \alpha_1\beta_1 \qquad (5.1.10)$$

But in reality, the considered DNA shows the completely different situation of pronounced inequality in the amplitudes of the probabilities of the nitrogenous bases C, A, T, P. These probabilities were shown above in Fig. 1.2: %C= 0.208499, %A = 0.291001, %T = 0.291756, %G = 0.208744. One can show corresponding amplitudes of the probabilities using their denotations from (5.1.4):

$$\gamma_{00} = (\%C)^{0.5} = 0.208499^{0.5} = 0.456617,$$
$$\gamma_{01} = (\%A)^{0.5} = 0.291001^{0.5} = 0.539445,$$
$$\gamma_{10} = (\%T)^{0.5} = 0.291756^{0.5} = 0.540144,$$
$$\gamma_{11} = (\%G)^{0.5} = 0.208744^{0.5} = 0.456885. \qquad (5.1.11)$$

Amplitudes of probabilities in the abstract case (5.1.9) and in reality (5.1.11) are significantly different that corresponding to the criterium (5.1.8) of the second considered option saying about quantum entanglement. This fact gives pieces of evidence that, in the human chromosomal DNA, its 2-qubit state |ψ$_{12}$> is entangled. It means that the 2-qubit state |ψ$_{12}$> of the composite quantum system cannot be divided into two separate, completely independent parts corresponding to two sequences of "amino- and keto-molecules" and "pyrimidine and purine molecules".

The result obtained on the quantum entanglement of the stochastic nucleotide sequence of the chromosomal DNA is important due to the key importance of the concept of entanglement for the entire quantum informatics as it was noted above.

Similar results about the existence of such entanglement were received for many other genomic DNAs analyzed by the author. These received results about the stochastic properties of genomic DNAs allow believing that molecular-genetic systems widely use a quantum entanglement (or a quantum-like entanglement) to provide their biological functions and that the topic of entanglement should be included in the future development of algebraic biology and the doctrine of evolution

based on bio-antenna arrays.

But what is about quantum entanglement in cases of presentations of genomic DNAs sequences as sequences of duplets, or sequences of triplets, or sequences of tetraplets, etc.? It turns out that in these cases you meet similar quantum entanglement again but for 2n-qubit quantum systems (n = 2, 3, 4, …). In other words, these 2n-qubit states of the composite quantum systems cannot be divided into separate, completely independent parts corresponding to two sequences of "amino- and keto-molecules" and "pyrimidine and purine molecules". It can be shown by analogy with the described case of the 1-textual presentations of single-stranded genomic DNA. Such quantum entanglements, realized in 1-, 2-, 3-, 4-textual representations of genomic DNAs sequences, have regular interrelations each with other, which are reflected in universal rules of stochastic organization of genomic DNAs and in a special family of algebraic equations using the Hadamard product (see their examples in Figs. 2.1 and 2.5).

In addition, we briefly note the following. We have just considered genetic qubits (5.1.2) and (5.1.3) built on the binary-opposition pairs "amino-keto" (C + A vs. G + T) and "pyrimidines-purines" (T+C vs. A+G). But the molecular DNA alphabet of four nucleotides is arranged by nature in such a way that it is endowed with another pair of binary-oppositional features associated with the complementarity of nitrogenous bases: in the DNA double-strand, the bases C and G are connected by 3 hydrogen bonds ("strong link"), and the bases A and T linked by 2 hydrogen bonds ("weak link"). Accordingly, it is also possible to consider genetic qubits built on this pair of oppositions "strong link - weak link". This leads to the possibility of a similar analysis of the 4-dimensional Hilbert space and 2-qubit systems arising on the following pairs of genetic qubits: 1) "amino-keto" and "strong bond-weak bond"; 2) "pyrimidine-purine" and "strong bond-weak bond". It turns out that in these 2-qubit representations of stochastic sequences of genomic DNAs, you also have appropriate quantum entanglements.

Now let's consider interrelations among the following 2n-qubit states (n = 1, 2, 3), which are represented by sets of probability amplitudes for 4 monoplets, 16 dublets, and 64 triplets in the case of the DNA sequence of human chromosome №1, whose probabilities are shown in Figs. 1.2 and 1.3 (we denote these 2n-qubit states by symbols $|\psi_4>$, $|\psi_{16}>$, and $|\psi_{64}>$ correspondingly; values are rounded to 4 decimal places):

$$|\psi_4> = 0.2085^{0.5}\,|00> + 0.2910^{0.5}\,|01> + 0.2918^{0.5}\,|10> + 0.2087^{0.5}\,|11> , \quad (5.1.12)$$

$$|\psi_{16}> = 0.0541^{0.5}\,|0000> + 0.0727^{0.5}\,|0001> + 0.0503^{0.5}\,|0010> + 0.0950^{0.5}\,|0011> +$$
$$+ 0.0713^{0.5}\,|0100> + 0.0103^{0.5}\,|0101> + 0.0743^{0.5}\,|0110> + 0.0714^{0.5}\,|0111> +$$
$$+ 0.0601^{0.5}\,|1000> + 0.0631^{0.5}\,|1001> + 0.0440^{0.5}\,|1010> + 0.0601^{0.5}\,|1011> +$$
$$+ 0.0957^{0.5}\,|1100> + 0.0729^{0.5}\,|1101> + 0.0505^{0.5}\,|1110> + 0.0542^{0.5}\,|1111> \quad (5.1.13)$$

$$|\psi_{64}> = 0.0138^{0.5}|000000>+0.0188^{0.5}|000001>+0.0152^{0.5}|000010>+0.0186^{0.5}|000011>$$
$$+ 0.0118^{0.5}\,|000100> + 0.0198^{0.5}\,|000101> + 0.0145^{0.5}\,|000110> + 0.0369^{0.5}\,|000111>$$
$$+ 0.0185^{0.5}\,|001000> + 0.0029^{0.5}\,|001001> + 0.0179^{0.5}\,|001010> + 0.0210^{0.5}\,|001011>$$
$$+ 0.0162^{0.5}\,|001100> + 0.0025^{0.5}|001101> + 0.0238^{0.5}|001110> + 0.0199^{0.5}\,|001111>$$
$$+ 0.0176^{0.5}|010000> + 0.0127^{0.5}|010001> + 0.0025^{0.5}|010010> + 0.0023^{0.5}|010011>$$
$$+ 0.0132^{0.5}|010100> + 0.0194^{0.5}|010101> + 0.0144^{0.5}|010110> + 0.0224^{0.5}|010111>$$
$$+ 0.0201^{0.5}|011000> + 0.0209^{0.5}|011001> + 0.0026^{0.5}|011010> + 0.0029^{0.5}|011011>$$
$$+ 0.0239^{0.5}|011100> + 0.0178^{0.5}|011101> + 0.0161^{0.5}|011110> + 0.0185^{0.5}|011111>$$

$+ 0.0159^{0.5}|100000> + 0.0196^{0.5}|100001> + 0.0110^{0.5}|100010> + 0.0199^{0.5}|100011>$
$+ 0.0125^{0.5}|100100> + 0.0146^{0.5}|100101> + 0.0096^{0.5}|100110> + 0.0196^{0.5}|100111>$
$+ 0.0223^{0.5}|101000> + 0.0023^{0.5}|101001> + 0.0194^{0.5}|101010> + 0.0128^{0.5}|101011>$
$+ 0.0144^{0.5}|101100> + 0.0025^{0.5}|101101> + 0.0133^{0.5}|101110> + 0.0176^{0.5}|101111>$
$+ 0.0197^{0.5}|110000> + 0.0198^{0.5}|110001> + 0.0146^{0.5}|110010> + 0.0195^{0.5}|110011>$
$+ 0.0096^{0.5}|110100> + 0.0112^{0.5}|110101> + 0.0126^{0.5}|110110> + 0.0160^{0.5}|110111>$
$+ 0.0372^{0.5}|111000> + 0.0188^{0.5}|111001> + 0.0199^{0.5}|111010> + 0.0190^{0.5}|111011>$
$+ 0.0145^{0.5}|111100> + 0.0153^{0.5}|111101> + 0.0119^{0.5}|111110> +$
$+ 0.0138^{0.5}|111111>$ (5.1.14)

One can calculate that the following inequalities hold for these 2n-qubit states (5.1.12 – 5.1.14):

- $|\psi_4> \otimes |\psi_4> \neq |\psi_{16}>$; (5.1.15)
- $|\psi_4> \otimes |\psi_{16}> \neq |\psi_{64}>$; (5.1.16)
- $|\psi_4> \otimes |\psi_4> \otimes |\psi_4> \neq |\psi_{64}>$. (5.1.17)

The inequality (5.1.15) testifies that the 4-qubit state $|\psi_{16}>$ cannot be expressed by the tensor product $|\psi_4> \otimes |\psi_4>$, that is, the state $|\psi_{16}>$ can be formally interpreted as quantum entangled regarding the states $|\psi_4>$.

The inequality (5.1.16) testifies that the 6-qubit state $|\psi_{64}>$ cannot be expressed by the tensor product $|\psi_4> \otimes |\psi_4> \otimes |\psi_4>$, that is, the state $|\psi_{64}>$ can be formally interpreted as quantum entangled regarding the states $|\psi_4>$.

The inequality (5.1.17) testifies that the 6-qubit state $|\psi_{64}>$ cannot be expressed by the tensor product $|\psi_4> \otimes |\psi_{16}>$, that is, the state $|\psi_{64}>$ can be formally interpreted as quantum entangled regarding the states $|\psi_4>$ and $|\psi_{16}>$.

Similar algebraic numerical data hold for different genomic DNAs and testify that genomic DNAs, as quantum (or quantum-like) systems, are vast multilevel networks of quantum entangled states.

- **5.2. The Hadamard product, nonlinear transformations in quantum computation, and the stochastic of genomic DNAs**

Quantum mechanics is fundamentally linear. Quantum computers are naturally well-suited to implementing linear operations. One of the important tasks for developing quantum computing and its applications is the general problem of implementing nonlinear transformations of quantum states. This problem is considered in a series of modern works by different authors, for example [Holmes et al., 2021; Guo, Mitarai, Fujii, 2021]. These works noted that nonlinear subroutines may prove key to a range of applications of quantum computing from solving nonlinear equations to data processing and quantum machine learning.

We showed above that the universal rules of stochastic organization of genomic DNAs are algebraically expressed by using the Hadamard product, which is used in the tensor-matrix theory of digital antenna arrays (Figs. 2.1 and 2.5). But the Hadamard product is also used in quantum computing tasks to create algorithms implementing basic nonlinear transformations of quantum states. The work [Holmes et al., 2021] introduces a notion of the "quantum Hadamard product", which uses to generate new sets of quantum states.

Let us return to the unexpected arising of the Hadamard product in algebraic expressions of universal interconnections between genetic probability matrices, whose

sums of entries are equal to 1 (see examples in Figs. 2.1 and 2.5). Note formal connections of these matrices with quantum 2n-qubits. For example, Fig. 2.1 shows the (2*2)-matrix of probabilities of 4 nucleotides in the 1-textual presentation of genomic DNAs [%C, %A; %T, %G], whose 4 entries can be interpreted as squares of probability amplitudes of the following 2-qubit system since their sum is equal to 1:

$$|\psi_{2q}\rangle = (\%C)^{0.5}|00\rangle + (\%A)^{0.5}|01\rangle + (\%T)^{0.5}|10\rangle + (\%G)^{0.5}|11\rangle \qquad (5.2.1)$$

where %C+%A+%T+%G =1.

Also Fig. 2.1 shows the (4*4)-matrix of probabilities of 16 duplets in the 2-textual presentation of genomic DNAs:
$$[\%CC, \%CA, \%AC, \%AA; \%CT, \%CG, \%AT, \%AG;$$
$$\%TC, \%TA, \%GC, \%GA; \%TT, \%TG, \%GT, \%GG],$$
whose 16 entries can be interpreted as squares of probability amplitudes of the following 4-qubit system since their sum is equal to 1:

$$|\psi_{4q}\rangle = (\%CC)^{0.5}|0000\rangle + (\%CA)^{0.5}|0001\rangle + (\%AC)^{0.5}|0010\rangle + (\%AA)^{0.5}|0011\rangle +$$
$$(\%CT)^{0.5}|0100\rangle + (\%CG)^{0.5}|0101\rangle + (\%AT)^{0.5}|0110\rangle + (\%AG)^{0.5}|0111\rangle +$$
$$(\%TC)^{0.5}|1000\rangle + (\%TA)^{0.5}|1001\rangle + (\%GC)^{0.5}|1010\rangle + (\%GA)^{0.5}|1011\rangle +$$
$$(\%TT)^{0.5}|1100\rangle + (\%TG)^{0.5}|1101\rangle + (\%GT)^{0.5}|1110\rangle + (\%GC)^{0.5}|1111\rangle,$$

where   %CC+%CA+%AC+%AA+%CT+%CG+%AT+%AG+
+%TC+%TA+%GC+ %GA+%TT+%TG+%GT+%GG = 1.   (5.2.2)

By analogy, the (8*8)-matrix (Fig. 2.5) of probabilities of 64 triplets in the 3-textual presentation of genomic DNAs can be interpreted as a matrix representation of the 6-qubit system.
In any of the tested genomic DNAs, these 2-qubit, 4-qubit, 6-qubit states turn out to be algebraically connected through using the Hadamard product of matrices (Fig. 2.1 and 2.5). Correspondingly, the genetic (2*2)-matrix of probabilities, representing a 2-qubit state, is nonlinearly transformed into the genetic (4*4)-matrix of probabilities, representing an appropriate 4-qubit state. So, the described author's analysis of universal rules of stochastic organization of genomic DNAs reveals the unexpected way of nonlinear transformations of quantum states, which - as far as we can judge – is unknown in works on quantum computing but fundamental for living Nature; this way connects quantum states of 2n-qubit systems in Hilbert spaces of different 2n-dimensions. It should be emphasized that this way of transformations of 2n-qubit states provides simultaneously quantum entanglement states as it was above noted.
The author believes that a discovery of this "genetic" way of such transformations of quantum states opens new perspectives for developing quantum algorithms and quantum computing in a close connection with bio-information patents of living nature. One can suppose that this way can lead, for example, to more biomorphic options of quantum machine learning.

-    **5.3. Universal stochastic rules of genomic DNAs and quantum informatics**

The matrix equalities in Figs. 2.1 and 2.5 can be represented in equivalent linear forms based on combinations of genetic 2-qubit states. It is the

phenomenological fact that the sum of all 4 entries in each of the mentioned tetra-multiplicating (2*2)-matrices (B_C, B_A, B_T, B_G, B_{CC}, B_{CA}, B_{CT}, B_{CG}, B_{AC}, B_{AA}, B_{AT}, B_{AG}, B_{TC}, B_{TA}, B_{TT}, B_{TG}, B_{GC}, B_{GA}, B_{GT}, B_{GG}) is equal to 1 with high accuracy as it was shown in Figs. 2.3 and 2.8 for the particular example of the DNA of human chromosome №1 (similar equalities hold for other tested genomic DNAs). Correspondingly, each of the noted genetic (2*2)-matrices can be interpreted as a matrix representation of an appropriate 2-qubit system. One can explain this by the following examples for the numeric matrices from Figs. 2.3 and 2.8 and equations (2.2-2.5) (numeric values are shown below for the DNA of human chromosome №1, rounded to 4 decimal places):

B_C = [%CC / %C, %CA / %C; %CT / %C, %CG / %C] =
   = [0.2594, 0.3489; 0.3422, 0.0494], which represents the following 2-qubit state:
$|\psi_{BC}\rangle$ = (%CC / %C)$^{0.5}$ |00> + (%CA / (%C)$^{0.5}$ |01> + (%CT / %C)$^{0.5}$ |10> +
      (%CG / %C)$^{0.5}$ |11> =
      = $0.2594^{0.5}$ |00> + $0.3489^{0.5}$ |01> + $0.3422^{0.5}$ |10> + $0.0494^{0.5}$ |11>;   (5.3.1)

B_A = [%AC / %A, %AA / %A; %AT / %A, %AG / %A] =
   = [0.1729, 0.3266; 0.2553, 0.2452], which represents the following 2-qubit state:
$|\psi_{BA}\rangle$ = (%AC / %A)$^{0.5}$ |00> + (%AA / (%A)$^{0.5}$ |01> + (%AT / %A)$^{0.5}$ |10> +
      (%AG / %A)$^{0.5}$ |11> =
      = $0.1729^{0.5}$ |00> + $0.3266^{0.5}$ |01> + $0.2553^{0.5}$ |10> + $0.2452^{0.5}$ |11>;   (5.3.2)

B_T = [%TC / %T, %TA / %T;   %TT / %T, %TG / %T] =
   = [0.2059, 0.2164; 0.3279, 0.2497], which represents the following 2-qubit state:
$|\psi_{BT}\rangle$ = (%TC / %T)$^{0.5}$|00> + (%TA / (%T)$^{0.5}$|01> + (%TT / %T)$^{0.5}$|10> +
      (%TG / %T)$^{0.5}$ |11> =
      = $0.2059^{0.5}$ |00> + $0.2164^{0.5}$ |01> + $0.3279^{0.5}$ |10> + $0.2497^{0.5}$ |11>;   (5.3.3)

B_G = [%GC / %G, %GA / %G;   %GT / %G, %GG / %G] =
   = [0.2109, 0.2878; 0.2417, 0.2596], which represents the following 2-qubit state:
$|\psi_{BG}\rangle$ = (%GC / %G)$^{0.5}$|00> + (%GA / (%G)$^{0.5}$|01> + (%GT / %G)$^{0.5}$|10> +
      (%GG / %G)$^{0.5}$ |11> =
      = $0.2109^{0.5}$ |00> + $0.2878^{0.5}$ |01> + $0.2417^{0.5}$ |10> + $0.2596^{0.5}$ |11>;   (5.3.4)

After the explanation of representations of the tetra-multiplicating (2*2)-matrices B_C, B_A, B_T, B_G by corresponding 2-qubits (5.3.1.-5.3.4), similar representations can be done by analogy regarding the 16 tetra-multiplicating (2*2)-matrices B_{CC}, B_{CA}, B_{CT}, B_{CG}, B_{AC}, B_{AA}, B_{AT}, B_{AG}, B_{TC}, B_{TA}, B_{TT}, B_{TG}, B_{GC}, B_{GA}, B_{GT}, B_{GG} (from Figs. 2.6-2.8). We show such representation only for the matrix B_{TG} for brief:

B_{TG} = [%TGC / %TG, %TGA / %TG; %TGT / %TG, %TGG / %TG] =
   = [0.2000, 0.2672; 0.2729, 0.2601], which represents the following 2-qubit state:
$|\psi_{BTG}\rangle$ = (%TGC / %TG)$^{0.5}$ |00> + (%TGA / %TG)$^{0.5}$ |01> + (%TGT / %TG)$^{0.5}$ |10>
      + (%TGG / %TG)$^{0.5}$ |11> =
      = $0.2000^{0.5}$ |00> + $0.2672^{0.5}$ |01> + $0.2729^{0.5}$ |10> + $0.2601^{0.5}$ |11>.   (5.3.5)

The lengths of all corresponding 4-dimensional vectors whose components are 4 probability amplitudes in such genetic 2-qubits are equal to 1, that is, they are equal

to each other. It means that these vectors form a single class of unitarily equivalent vectors: each of these vectors can be transformed into another vector of this class by unitary transformations (or orthogonal transformations in the case of real components) since unitary transformations of vectors preserve their lengths. It is interesting since all calculations in quantum computers are based on precisely unitary transformations. Accordingly, the revealed multifaceted relationship between the features of the stochastic organization of genomic DNAs and unitary (orthogonal) transformations is another evidence of the deep conjugation of molecular genetics with the formalisms of quantum mechanics and quantum informatics.

The matrix of probabilities of nucleotides in 1-textual presentation of the considered DNA (Fig. 1.2) represents the following 2-qubit state $|\psi_{CATG}\rangle$ as well:

[%C, %A; %T, %G] = [0.208499, 0.291001; 0.291756, 0.208744],
$|\psi_{CATG}\rangle = (\%C)^{0.5}|00\rangle + (\%A)^{0.5}|01\rangle + (\%T)^{0.5}|10\rangle + (\%G)^{0.5}|11\rangle =$
$= 0.208499^{0.5}|00\rangle + 0.291001^{.5}|01\rangle + 0.291756^{0.5}|10\rangle + 0.208744^{0.5}|11\rangle$ (5.3.6)

Now let us express the matrix equality from Figs. 2.1 by an equivalent linear form based on combinations of the described genetic 2-qubits using the tensor product. Let's start with the 2-qubit $|\psi_{CATG}\rangle$ (5.3.6) of the probability amplitudes of the 4 nucleotides in a 1-textual representation of a long single-stranded DNA:

$|\psi_{CATG}\rangle = (\%C)^{0.5}|00\rangle + (\%A)^{0.5}|01\rangle + (\%T)^{0.5}|10\rangle + (\%G)^{0.5}|11\rangle$ (5.3.7)

Then tensor multiply each of the 4 terms of this 2-qubit $|\psi_{CATG}\rangle$ by the corresponding 2-qubit from the family of four 2-qubits $|\psi_{BC}\rangle$, $|\psi_{BA}\rangle$, $|\psi_{BT}\rangle$ and $|\psi_{BG}\rangle$ (5.3.1-5.3.4) as it is shown in (5.3.8):

$(\%C)^{0.5}|00\rangle \otimes |\psi_{BC}\rangle + (\%A)^{0.5}|01\rangle \otimes |\psi_{BA}\rangle + (\%T)^{0.5}|10\rangle \otimes |\psi_{BT}\rangle +$
$+ (\%G)^{0.5}|11\rangle \otimes |\psi_{BG}\rangle =$
$= (\%C)^{0.5}|00\rangle \otimes \{(\%CC / \%C)^{0.5}|00\rangle + (\%CA / (\%C)^{0.5}|01\rangle + (\%CT / \%C)^{0.5}|10\rangle +$
$(\%CG / \%C)^{0.5}|11\rangle\} + (\%A)^{0.5}|01\rangle \otimes \{(\%AC / \%A)^{0.5}|00\rangle + (\%AA / (\%A)^{0.5}|01\rangle +$
$(\%AT / \%A)^{0.5}|10\rangle + (\%AG / \%A)^{0.5}|11\rangle\} + (\%T)^{0.5}|10\rangle \otimes \{(\%TC / \%T)^{0.5}|00\rangle +$
$(\%TA / (\%T)^{0.5}|01\rangle + (\%TT / \%T)^{0.5}|10\rangle + (\%TG / \%T)^{0.5}|11\rangle\} +$
$+ (\%G)^{0.5}|11\rangle \otimes \{(\%GC / \%G)^{0.5}|00\rangle + (\%GA / (\%G)^{0.5}|01\rangle + (\%GT / \%G)^{0.5}|10\rangle +$
$+ (\%GG / \%G)^{0.5}|11\rangle\} =$
$= (\%CC^{0.5}|0000\rangle + \%CA^{0.5}|0001\rangle + \%CT^{0.5}|0010\rangle + \%CG^{0.5}|0011\rangle) +$
$+ (\%AC^{0.5}|0100\rangle + \%AA^{0.5}|0101\rangle + \%AT^{0.5}|0110\rangle + \%AG^{0.5}|0111\rangle) +$
$+ (\%TC^{0.5}|1000\rangle + \%TA^{0.5}|1001\rangle + \%TT^{0.5}|1010\rangle + \%TG^{0.5}|1011\rangle) +$
$+ (\%GC^{0.5}|1100\rangle + \%GA^{0.5}|1101\rangle + \%GT^{0.5}|1110\rangle + \%GG^{0.5}|1111\rangle)$ (5.3.8)

Let us verify that the use of component-wise tensor multiplication by 2-qubits $|\psi_{BC}\rangle$, $|\psi_{BA}\rangle$, $|\psi_{BT}\rangle$, and $|\psi_{BG}\rangle$ in (5.3.8) automatically ensures that the phenomenological rules (2.5) hold for genomic DNAs. Let's show this execution for equality in the first line in (2.5): %C ≈ %CC+%CA+%CT+%CG. Using (5.3.8), corresponding to the 16-dimensional Hilbert space, we calculate in its 4-dimensional subspace the square of the length of the vector corresponding to the expression $\%CC^{0.5}|0000\rangle + \%CA^{0.5}|0001\rangle + \%CT^{0.5}|0010\rangle + \%CG^{0.5}|0011\rangle$. This square of length L^2 is equal to the sum of the squares of the coordinates of the given vector:

$$L^2 = \%CC + \%CA + \%CT + \%CG =$$
$$= \%C * \{(\%CC / \%C) + (\%CA / \%C) + (\%CT / \%C) + (\%CG / \%C)\} = \%C \quad (5.3.9)$$

In expression (5.3.9), the sum of the terms in curly brackets is equal to 1, since it represents the sum of the squared probability amplitudes from the 2-qubit $|\psi_{BC}>$ (5.3.1). Hence, as a result of the described tensor operation, we obtain, in the language of formalisms of quantum informatics, the verifiable equality $\%C = \%CC + \%CA + \%CT + \%CG$, which now represents the metric relation of equality of the lengths of the considered vectors in 4-dimensional and 16-dimensional Hilbert spaces.

Thus, expressions (5.3.7) and (5.3.8), referring respectively to vectors in 4-dimensional and 16-dimensional Hilbert spaces, show a numerical relationship between the considered sets of phenomenological probabilities of 4 monoplets and 16 duplets in the considered representation of genomic DNAs. We emphasize that in this case, we expressed the desired relationship between the two described sets of probabilities 4 monoplets and 16 duplets in genomic DNAs without using the Hadamard product operation for matrices, replacing it with a specific component-by-component tensor multiplication by 2-qubits. This makes it possible to model in the language of metric relations and quantum information formalisms the universal rules of the stochastic organization of genomic DNAs described above, examples of which are given by expressions (2.5) and (2.8) and which are reduced to algorithmic tensor combinations of 2-qubit systems.

The set of 16 computational basic states $|0000>$, $|0001>$, …, $|1111>$ specified in (5.3.8) defines a (4*4)-table, in which the rows are binary numbered by the first two digits of these binary expressions, and the columns are binary numbered by their last two digits, as shown in Fig. 5.3.1.

At the same time, the corresponding probability amplitudes or the probabilities of these computational basic states are uniquely entered into each cell of the table. The resulting table of probabilities for these 16 computational base states of a 4-qubit is structurally similar to the DNA alphabet matrix of 16 duplets and the probability matrix of 16 duplets shown at the beginning of the article in Fig. 1.1 and 1.2.

	00	01	10	11
00	%CC	%CA	%AC	%AA
01	%CT	%CG	%AT	%AG
10	%TC	%TA	%GC	%GA
11	%TT	%TG	%GT	%GG

Fig. 5.3.1. The table of probabilities of 16 computational basis states of the 4-qubit system (5.3.8), corresponds to percentage values of 16 duplets in the 2-textual representation of any genomic DNA nucleotide sequence.

Similarly, using this 4-qubit containing the probability amplitudes of 16 duplets (5.3.8), and component-by-component tensor-multiplying its 16 computational base states by 2-qubit representations of the corresponding 16 tetra-multiplicating (2*2)-matrices B_{CC}, B_{CA}, B_{CT}, B_{CG}, B_{AC}, B_{AA}, B_{AT}, B_{AG}, B_{TC}, B_{TA}, B_{TT}, B_{TG}, B_{GC}, B_{GA}, B_{GT}, B_{GG} (from Figs. 2.6-2.8), you end up with a 64-qubit; raising to the second power the amplitudes of the probabilities of its 64 computational basis states, you get the phenomenological values of the probabilities of 64 triplets in a 3-

text representation of genomic DNAs.

In the general case, the relationship between the probabilities of n-plets and (n+1)-plets in n-text and (n+1)-text representations of genomic DNAs is expressed for each concrete genomic DNA by the following general algorithm based on quantum information formalisms and generalizing expression (5.3.8):

- using a 2n-qubit representing the probability amplitudes of n-plets in the considered genomic DNA, and applying the component-by-component tensor product of each of its 4^n computational basis states by 2-qubits corresponding to 4^n tetra-multiplicating (2*2)-matrices of probabilities, you get a 2(n+1)-qubit representing the probability amplitudes of (n+1)-plets in that DNA (n = 1, 2, 3, 4, …, but much small than the DNA length).

This multiple uses of 2-qubits, which have four computational basis states, models the phenomenological tetra-structuring relations, according to which, in n-textual and (n+1)-textual representations of genomic DNAs, the probability of any n-plet is equal to the sum of the probabilities of four (n+1)-plets [Petoukhov, 2021c] (here n = 1, 2, 3, 4, ... is relatively small). Examples of these tetra-relations are the following equalities, the fulfillment of which for the case of DNA of human chromosome No. 1 can be verified using the probability values from Figs. 1.2-1.4:

$$\%C \approx \%CC + \% \ CA + \%CT + \%CG$$
$$\%CA \approx \%CAC + \% \ CAA + \%CAT + \%CAG;$$
$$\%CAC \approx \%CACC + \% \ CACA + \%CACT + \%CACG; \ etc. \qquad (5.3.10)$$

Similar tetra-relations, penetrating the stochastic organization of genomic DNAs and associated with 2-qubits of quantum informatics, are conveniently visualized in graphic forms of multi-tiered mandalas, which are described in the next section.

6. Mandalas and universals of the stochastic organization of genomic DNAs

Many authors have long drawn attention to the fact that the family of DNA-alphabets, which contain 4 nucleotides, 4^2 duplets, 4^3 triplets, etc. conveniently visualized in 4-section pie charts like the one shown in Fig. 6.1. Similar 4-section pie charts are called sometimes mandalas since they resemble ancient mandala images, which are used for thousands of years by millions of Buddhists, Hindus, and other believers as a meditation tool to achieve "enlightenment" and healing. One can see examples of such tiered mandalas of the family of DNA alphabets on websites https://www.researchgate.net/figure/Genetic-code-Wikipedia_fig1_338865739, https://www.pinterest.com/pin/350647520964620594/, http://www.kozlenkoa.narod.ru/gencode1.htm, etc. In particular, tiered mandalas of DNA-alphabets are connected with Yin-Yang schemes of the Ancient Chinese book "I-Ching" [https://wiki.deldebbio.com.br/index.php?title=File:Knowledge-iching-mandala.jpg].
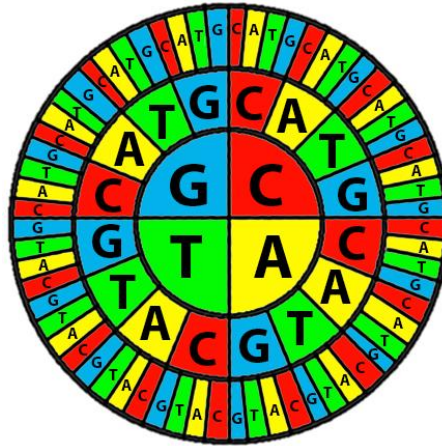
Fig. 6.1. A graphic representation of the family of interrelated DNA-alphabets of 4 nucleotides, 4^2 duplets, and 4^3 triplets as a tiered pie chart having 4 sectors. The first tier contains 4 nucleotides C, A, T, G. The second tier contains 16 duplets, whose appropriate second letters are shown. The third tier contains 64 triplets whose appropriate third letters are shown.

By analogy let us create now mandalas not for DNA-alphabets but for genomic probabilities of n-plets in n-textual representations of genomic DNAs. In such a mandala, each of its cellules contains a percentage of an appropriate n-plet in the considered DNA (instead of the n-plet symbol shown in Fig. 6.1). More precisely, the first tier contains percentages %C, %A, %T, %G of 4 nucleotides in the 1-textual representation of the considered DNA; the second tier contains percentages of 16 duplets (%CC, %CA, %CT, %CG, ….) in the 2-textual representation of the DNA; the third tier contains percentages of 64 triplets (%CCC, %CCA, %CCT, …) in the 3-textual representation of the DNA (this article describes only a case of genomic probability mandalas for values n = 1, 2, 3 though cases of higher values n can be considered as well). In these mandalas, the angular width of each cellule is proportional to the percent value of the corresponding n-plet, that is, on each tier, its cellules differ in angular width (in contrast to the DNA-alphabets mandala in Fig. 6.1, in which all cellular of one tier are the same in angular width).

Families of probabilities of 4 nucleotides, 16 duplets, and 64 triplets in genomic DNAs are connected correspondingly with 2-qubit, 4-qubit, and 6-qubit states $|\psi_4\rangle$, $|\psi_{16}\rangle$, $|\psi_{64}\rangle$ as it was noted in expressions (5.1.12-5.1.14):

$$|\psi_4\rangle = \sqrt{\%C}\,|00\rangle + \sqrt{\%A}\,|01\rangle + \sqrt{\%T}\,|10\rangle + \sqrt{\%G}|\,11\rangle \qquad (6.1)$$

$$\begin{aligned}|\psi_{16}\rangle = {}& \sqrt{\%CC}\,|0000\rangle + \sqrt{\%CA}\,|0001\rangle + \sqrt{\%CT}\,|0010\rangle + \sqrt{\%CG}\,|0011\rangle + \\ & + \sqrt{\%AC}\,|0100\rangle + \sqrt{\%AA}\,|0101\rangle + \sqrt{\%AT}\,|0110\rangle + \sqrt{\%AG}\,|0111\rangle + \\ & + \sqrt{\%TC}\,|1000\rangle + \sqrt{\%TA}\,|1001\rangle + \sqrt{\%TT}\,|1010\rangle + \sqrt{\%TG}\,|1011\rangle + \\ & + \sqrt{\%GC}\,|1100\rangle + \sqrt{\%GA}\,|1101\rangle + \sqrt{\%GT}\,|1110\rangle + 0\sqrt{\%GG}\,|1111\rangle \quad (6.2)\end{aligned}$$

$$\begin{aligned}|\psi_{64}\rangle = {}& \sqrt{\%CCC}\,|000000\rangle + \sqrt{\%CCA}\,|000001\rangle + \sqrt{\%CCT}\,|000010\rangle + \sqrt{\%CCG}\,|000011\rangle \\ & + \sqrt{\%CAC}\,|000100\rangle + \sqrt{\%CAA}\,|000101\rangle + \sqrt{\%CAT}\,|000110\rangle + \sqrt{\%CAG}\,|000111\rangle \\ & + \sqrt{\%CTC}\,|001000\rangle + \sqrt{\%CTA}\,|001001\rangle + \sqrt{\%CTT}\,|001010\rangle + \sqrt{\%CTG}\,|001011\rangle \\ & + \sqrt{\%CGC}\,|001100\rangle + \sqrt{\%CGA}\,|001101\rangle + \sqrt{\%CGT}\,|001110\rangle + \sqrt{\%CGG}\,|001111\rangle \\ & + \sqrt{\%ACC}\,|010000\rangle + \sqrt{\%ACA}\,|010001\rangle + \sqrt{\%ACT}\,|010010\rangle + \sqrt{\%ACG}\,|010011\rangle\end{aligned}$$

$$+ \sqrt{\%AAC} |010100> + \sqrt{\%AAA} |010101> + \sqrt{\%AAT} |010110> + \sqrt{\%AAG} |010111>$$
$$+ \sqrt{\%ATC} |011000> + \sqrt{\%ATA} |011001> + \sqrt{\%ATT} |011010> + \sqrt{\%ATG} |011011>$$
$$+ \sqrt{\%AGC} |011100> + \sqrt{\%AGA} |011101> + \sqrt{\%AGT} |011110> + \sqrt{\%AGG} |011111>$$
$$+ \sqrt{\%TCC} |100000> + \sqrt{\%TCA} |100001> + \sqrt{\%TCT} |100010> + \sqrt{\%TCG} |100011>$$
$$+ \sqrt{\%TAC} |100100> + \sqrt{\%TAA} |100101> + \sqrt{\%TAT} |100110> + \sqrt{\%TAG} |100111>$$
$$+ \sqrt{\%TTC} |101000> + \sqrt{\%TTA} |101001> + \sqrt{\%TTT} |101010> + \sqrt{\%TTG} |101011>$$
$$+ \sqrt{\%TGC} |101100> + \sqrt{\%TGA} |101101> + \sqrt{\%TGT} |101110> + \sqrt{\%TGG} |101111>$$
$$+ \sqrt{\%GCC} |110000> + \sqrt{\%GCA} |110001> + \sqrt{\%GCT} |110010> + \sqrt{\%GCG} |110011>$$
$$+ \sqrt{\%GAC} |110100> + \sqrt{\%GAA} |110101> + \sqrt{\%GAT} |110110> + \sqrt{\%GAG} |110111>$$
$$+ \sqrt{\%GTC} |111000> + \sqrt{\%GTA} |111001> + \sqrt{\%GTT} |111010> + \sqrt{\%GTG} |111011>$$
$$+ \sqrt{\%GGC}|111100>+\sqrt{\%GGA}|111101>+\sqrt{\%GGT}|111110>+\sqrt{\%GGG}|111111>   \quad (6.3)$$

From the standpoint of 2n-qubit states of genomic DNAs (6.1-6.3), the genomic probability mandalas can be called "quantum information mandalas" presenting genomic stochastics. In particular, these mandalas reflect quantum entanglements, which exist in the stochastic organization of genomic DNAs as it was noted in paragraph 5.1. Fig. 6.2 represents the quantum information mandala of DNA of human chromosome №1 whose n-plet percentages and corresponding 2n-qubit states are shown above in expressions (5.1.12-5.1.14).
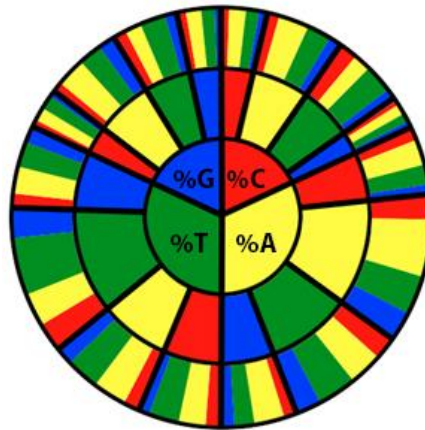

Fig. 6.2. The quantum information mandala of DNA of human chromosome №1 (this image was done by the author).

One should note the following features of the quantum information mandala in Fig. 6.2:

- 1) An angular width of any cellule of the first tier is practically equal to the sum of angular widths of 4 appropriate cellules of the second tier since %N ≈ %NC + %NA + %NT + %NG, where N refers to any of nucleotides C, A, T, G;
- 2) An angular width of any cellule of the second tier is practically equal to the sum of angular widths of 4 appropriate cellules of the third tier in accordance with the described phenomenological rules of genomic stochastics [Petoukhov, 2020a-c, 2021a].

Various genomes can significantly differ each other by n-plet probabilities in their genomic DNAs. Correspondingly their quantum information mandalas differ each

from other. Each genomic DNA is characterized by its individual quantum information mandala, which reflect individual features of its system of quantum entanglements. Fig. 6.3 shows examples of quantum information mandalas of some eukaryotic and prokaryotic genomic DNA.
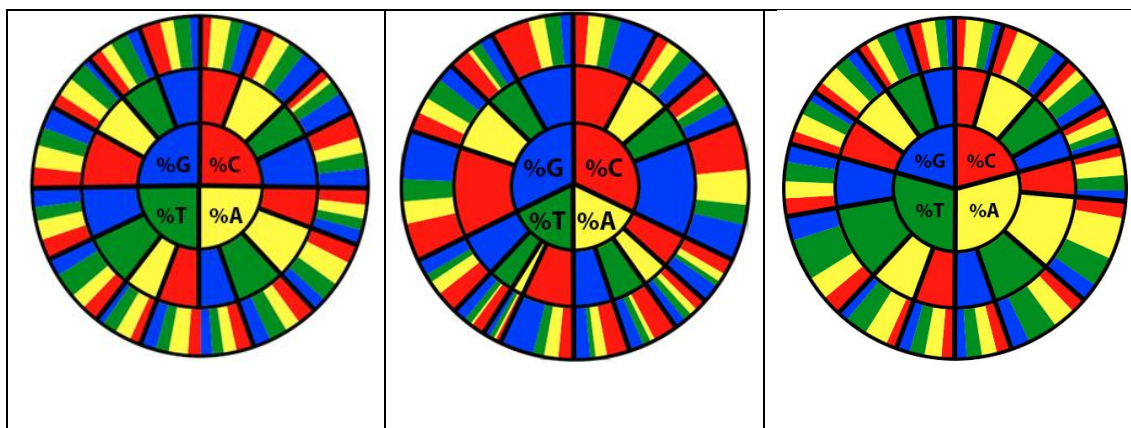

Fig. 6.3. Examples of quantum information mandalas of eukaryotic and prokaryotic genomic DNAs. **Left**: bacteria *Escherichia coli* CFT073, complete genome, GenBank: AE014075.1, 5231428 bp, (initial data taken from https://www.ncbi.nlm.nih.gov/nuccore/AE014075.1?report=genbank).
Middle: rhizobacteria *Bradyrhizobium japonicum* strain E109, complete genome, 9224208 bp (initial data taken from https://www.ncbi.nlm.nih.gov/nuccore/CP010313.1?report=genbank).
Right: fruit fly *Drosophila melanogaster* chromosome 2L, NCBI Reference Sequence: NT_033779.5 LOCUS NT_033779 23513712 bp (initial data taken from https://www.ncbi.nlm.nih.gov/nuccore/NT_033779.5).

But the author's comparative analysis of different chromosomes of eukaryotic genomes reveal that in each of the tested genomes quantum information mandalas of its chromosomes are very similar to each other. Figs. 6.2 and 6.4 confirm this observation by examples of similarities of quantum information mandalas of human somatic and sex chromosomes. In particular, this gives some pieces of evidence that different chromosomes of the same eukaryotic genome have similar quantum entanglements and form a single system of quantum (or quantum-like) entanglements.
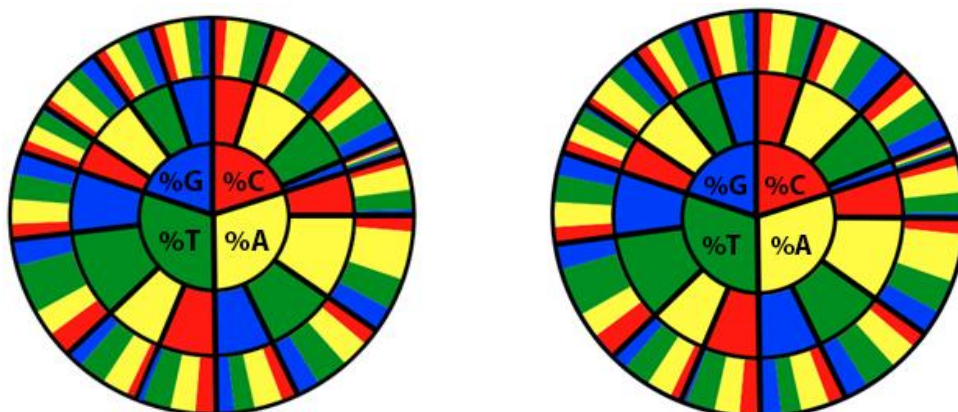
Fig. 6.4. Quantum information mandalas of stochastic organization of human sex chromosomes X (at left) and Y (at right).

We briefly note else that the phenomenological rules of stochastic organization of genomic DNAs provide an opportunity to build for each of the 16 duplets or each of the 64 triplets its mandala since this stochastic organization of genomic DNAs possesses fractal-like features [Petoukhov, 2020a-c, 2021a]. Correspondingly each genomic DNA can be considered as a system of many interrelated quantum information mandalas.

We suppose that the mandala-like organization of eukaryotic and prokaryotic genomes relates to the ancient psychologic theme of mandalas, which were used as meditation tools to achieve "enlightenment" and healing by millions of Buddhists, Hindus, and other believers. The creator of analytical psychology K. Jung and his collaborator Nobel laureate in physics W. Pauli considered the mandala to be an innate archetype of the unconscious and the conjugation of a cosmogram with a psychogram, capable of harmonizing the psyche. It can be added that millennia of the practice of mandala meditation are associated with the idea of musical harmony, reflected, in particular, in the rows of scalable bells in ancient Buddhist monasteries. Ancient teachings from the "enlightened" sages of India, China, and other countries asserted the view of musical harmony as something primordial.

In our time some kinds of music are used in biotechnological processes (for example, in the wine-producing and stimulation of growth of plants), musical therapy, etc. The author develops adequate - from a genetic point of view - methods of the musical sounding of quantum information mandalas of various genomes to get "genomic quantum information music", which could reflect in particular quantum entanglements of the considered genomic DNAs and which can be usefully applied in different fields: biotechnologies, regenerate medicine, musical therapy, improvements of ancient technologies of mandala-musical meditations for enlightenment and healing. The issues of the affinity of the genetic harmony of organisms with musical harmony are studied with the participation of the author in the special "Center for Interdisciplinary Research of Musical Creativity" of the Moscow State Conservatory. P.I. Tchaikovsky (existing since 2012, http://www.mosconsv.ru/ru/groups.aspx?id=135683).

Some concluding remarks

The scientific community has long discussed the relationship between innate knowledge and knowledge acquired in the course of life. The extreme point of view is formulated in Plato's famous statement that to know means to remember, awakening, as it were, from sleep. In particular, Kepler was a supporter of this point of view; it is described in detail in the article by the Nobel laureate in physics W. Pauli [Pauli, 1948]. Close to this is the widespread opinion that our body, with its nervous system and everything else, already carries in hidden forms the fullness of knowledge, whose parts come into our consciousness when they are insistently requested. But our body grows from a single fertilized cell carrying a genome with DNA and RNA molecules. It is obvious that this original cell, together with its genome, cannot contain all the named completeness of knowledge. But then additional knowledge should come gradually in the course of ontogeny to the developing multicellular organism from outside. In this case, it is the systems of bio-antenna arrays that can serve as the

system through which cosmic and planetary wave energy-informational influences enter the body from the outside world; these external influences are necessary for the adequate development and replenishment of the body's knowledge.

From the point of view of the stated doctrine, biological evolution can be formally considered as the evolution of systems of digital bio-antenna arrays to increase the efficiency of communications between the parts of the body and with the outside world. At the same time, communication orientation appears in evolution. The factor of increasing the possibilities of such communication can be considered a system-forming factor in biology according to the theory of P.K. Anokhin [Anokhin, 1978]. It is possible to develop the concept of "digital antenna biology and biological evolution" with access to a more general concept of the "antenna universe", which understands the world as a system of digital antennas distributed randomly and non-randomly.

Antenna arrays can be made from different chemical materials but perform similar functions. The radiations of antenna arrays can be the same even if the antennas are made of different materials. It is just as the same codes can work with transceivers made of different materials or as the same theory of resonances is applied to different antenna systems.

The topic of antenna arrays turns out to be cross-cutting for all levels of biological organization - from the genomes of higher and lower organisms to inherited sensory and other life support systems, including those associated with intellectual activity. Because of this, the presented doctrine is useful as a unifying platform for considering biological phenomena of different levels from a unified point of view, the development of algebraic and quantum biology, as well as for applied work on organ regeneration, medical diagnostics, artificial intelligence, etc.

At present, humanity is intensively encircling the Earth with technical antenna arrays on land, underwater, in the air, and space. From the point of view of the stated doctrine of bio-antenna arrays, this activity can be considered as a system modification of the Earth according to the bio-antenna arrays system image and likeness of a living organism.

People are used to writing and reading texts in a form of separate lines. In television, a two-dimensional image is transmitted by the horizontal scanning method, which represents this image as a sequence of running lines. In genomic DNAs, we meet with a radically different way of recording information, which uses a multi-layered system of parallel texts, each of which is based on its individual alphabet. This system has emergent properties that constitute the information patents of wildlife and are currently being studied in connection with applied problems.

The stochastic organization of genomic DNAs must give pieces of evidence about special interconnections between formalisms of antenna arrays and formalisms of quantum informatics described above. Correspondingly the doctrine of evolution on bio-antenna arrays is connected with formalisms of quantum informatics and quantum mechanics. Data were revealed on quantum (or quantum-like) entanglements in the stochastic organization of these DNAs. These data open new approaches to understanding the role of quantum entanglements in the inherited being of organisms.

Acknowledgments

References

Albert J. S., Crampton W. G. Electroreception and Electrogenesis. In: Lutz, P. L. (ed.). *The Physiology of Fishes*. Boca Raton, FL: CRC Press. pp. 429–470 (2006). ISBN 9780849320224.

Anokhin P.K. *Selected works. Philosophical aspects of the theory of a functional system*. - M., Nauka (1978, in Russian).

Ball Ph. Schrödinger's cat among biology's pigeons: 75 years of *What Is Life?* – Nature, v. 560, p.548-550, August 2018.

Blau S. Light as a Feather: Structural Elements Give Peacock Plumes Their Color. *Physics Today*, 57, 1, 18 (2004); DOI: 10.1063/1.1650059, https://physicstoday.scitation.org/doi/pdf/10.1063/1.1650059

Blekhman I.I., *Vibrational mechanics*. Singapore: World Scientific, 509 p. (2000).

Blekhman I.I., Vibration "changes the laws of mechanics"*, Priroda*, No. 11 (2003, in Russian), http://vivovoco.astronet.ru/VV/JOURNAL/NATURE/11_03/VIBRATION.HTM

Bullock T.H., Hamstra Jr. R., Scheich H. The jamming avoidance response of high frequency electric fish. J. Comp. Physiol. 77, pp. 1-22 (1972).

Ganiev R.F., Ganiev S.R., Kasilov V.P., Pustovgar A.P. *Wave technology in mechanical engineering*. Massachusetts: Scrivener Publishing LLC (2015).

Cook T.A. *The Curves of Life*. London: Constable and Co, 1914.

Denisova O.A., Scaldin O.A. Piezoelectric effect in liquid crystals. *Electrical and data processing facilities and systems*, № 4, v. 9, p. 145-153, 2013, https://cyberleninka.ru/article/n/piezoelektricheskiy-effekt-v-zhidkih-kristallah

Dolgaleva K., Wei S.K., Lukishova S.G., Chen S.H., Schwertz K., Boyd R.W. Enhanced laser performance of cholesteric liquid crystals doped with oligofluorene dye. *Journal of the Optical Society of America*. **25** (9): 1496–1504 (2008). Bibcode:2008JOSAB..25.1496D. doi:10.1364/JOSAB.25.001496

Durant F., Bischof J., Fields C., Morokuma J., LaPalme J., Hoi A., Levin M. The Role of Early Bioelectric Signals in the Regeneration of Planarian Anterior/Posterior Polarity). *Biophysical Journal*, v. 116, issue 5, pp. 948-961, 5 March 2019.

Feltz B., Crommelink M., Goujon Ph. *Self-organization and emergence in life sciences*. p.1, Springer Nature Switzerland AG (2006). ISBN: 978-90-481-6997-9

Fraccia, T., Smith, G., Zanchetta, G., et al. Abiotic ligation of DNA oligomers templated by their liquid crystal ordering. *Nat Commun* **6,** 6424 (2015).

Flack H.D. Louis Pasteur's discovery of molecular chirality and spontaneous resolution in 1848, together with a complete review of his crystallographic and chemical work. *Acta Crystallographica*, Section A, vol. 65, pp. 371–389 (2009).

Fröhlich H. Introduction. Theoretical Physics and Biology. – In: H. Fröhlich, editor *Biological Coherence and Response to External Stimuli*, p. 3-24 (Springer, 1988), ISBN 978-0-387-18739-6.

Fujikake H., Takizawa K., Aida T., Negishi T., Kobayashi M. Video camera system using liquid-crystal polarizing filter to reduce reflected light. - *IEEE Transactions on Broadcasting*. **44** (4): 419 (1998). doi:10.1109/11.735903

Günther M., Klotz L. Schur's theorem for a block Hadamard product. - Linear Algebra and its Applications, 437 (2012) 948–956, http://dx.doi.org/10.1016/j.laa.2012.04.002

Guo N., Mitarai K., Fujii K. Nonlinear transformation of complex amplitudes via quantum singular value transformation. arXiv:2107.10764v1 [quant-ph] (22 Jul 2021).

Gupta M., Sarangi B.R., Deschamps J., Nematbakhsh Y., Callan-Jones A., Margadant F., Mege R. M., Lim C. T., Voituriez R., Ladoux B. *Nat Commun*, 6, 7525 (2015).

Harroun S.G., Lauzon D., Ebert M., Desrosiers A., Wang X., Vallée-Bélisle A. Monitoring protein conformational changes using fluorescent nanoantennas. – *Nature Methods*, v. 19, p. 71-80 (January 2022). https://doi.org/10.1038/s41592-021-01355-5

Hasan Md.R., Helleso Ol.G. Dielectric optical nanoantennas. *Nanotechnology*, vol. 32, № 20, 202001 (2021), https://iopscience.iop.org/article/10.1088/1361-6528/abdceb#back-to-top-target.

Herman M.A. *Semiconductor Superlattices*. Akademie-Verlag, 1986.

Holmes Z., Coble N., Sornborger A.T., Subasi Y. On nonlinear transformations in quantum computation. arXiv:2112.12307v1 [quant-ph] (23 Dec 2021).

Hopkins C. D. Design features for electric communication. - *Journal of Experimental Biology*, 202 (Pt 10), pp. 1217–1228 (1999). doi:10.1242/jeb.202.10.1217. PMID 10210663

Horn R.A., Johnson C.R. *Matrix analysis*. Cambridge University Press (2012).

Hui W., Ke-Qin Zh. Photonic crystal structures with tunable structure color as colometric sensors. - *Sensors*. **13** (4): 4192–4213 (2013). doi:10.3390/s130404192. PMC 3673079. PMID 23539027

Joannopoulos J.D., Johnson S.G., Winn J.N., Meade R.D. *Photonic Crystals: Molding the Flow of Light* (2nd ed.), (2008), ISBN 978-0-691-12456.

Kopp V.I, Fan B., Vithana H.K., Genack A.Z. "Low-threshold lasing at the edge of a photonic stop band in cholesteric liquid crystals". *Optics Letters*. **23** (21), pp. 1707–9. (1998). doi:10.1364/OL.23.001707. PMID 18091891

Krasnok A.E., Maksymov I.S., Denisyuk A.I, Belov P.A., Miroshnichenko A.E., Simovskii C.R., Kivshar Yu.S. Optical nanoantennas. - *Phys. Usp*. **56**, pp.539–564 (2013). DOI: 10.3367/UFNe.0183.201306a.0561 , https://iopscience.iop.org/article/10.3367/UFNe.0183.201306a.0561.

Leo V. How it works. Dolphin echolocation. – https://www.stena.ee/blog/kak-eto-rabotaet-eholokatsiya-delfinov , December 11, 2015 (in Russian)

Levin M. The electrical blueprints that orchestrate life. *A video interview* (2020), https://www.youtube.com/watch?v=XheAMrS8Q1c

Levin M., Martyniuk Ch.J. The bioelectric code: An ancient computational medium

for dynamic control of growth and form. - *Biosystems*. 164, p. 76-93 (2018 Feb). DOI: 10.1016/j.biosystems.2017.08.009.

Lieberman E.A., Minina S.V., Moshkov D.A., Santalova I.M., Chistopolsky I.A., Shklovsky-Kordy N.E. Experimental verification of the role of the cytoskeleton in solving the problems facing the animal brain by the neuron. Biochemistry, Vol. 73, Issue 4, pp. 587-591 (2008). ISSN: 0320-9725

McLaughlin K. A., Levin M. Bioelectric signaling in regeneration: mechanisms of ionic controls of growth and form. - *Dev. Biol*. 433:177–189 (2018).

Milligan Th. A. *Modern Antenna Design*. 2nd Ed., John Wiley & Sons (2005), ISBN 0471720607

Minochkin A.I., Rudakov V.I., Slyusar V.I. *Fundamentals of military-technical research. Theory and applications.* - Volume 2: *Synthesis of an information support tools for weapons and military equipment.* Kyiv (2011). ISBN 978-966-2726-00-8, ISBN 978-966-2726-04-06 (vol. 2.) (in Russian).

Nielsen M.A., Chuang I.L. *Quantum Computation and Quantum Information*. New York: Cambridge Univ. Press. (2010).

Nikandrov V.V. Inorganic semiconductors in biological and biochemical systems: biosynthesis, properties, and photochemical activity. - *Advances in biological chemistry*, vol. 40, p. 357-396 (2000, in Russian).

Norman L.J., Dodsworth C., Foresteire D., Thaler L. Human click-based echolocation: Effects of blindness and age, and real-life implications in a 10-week training program. – *PloS ONE* 16(6): e0252330 (2021)

Pavelyev A.G., Wickert J., Torsten S., Gubenko V.N., Matyugov S.S., Pavelyev A.A. Radio holographic methods for atmospheric, ionospheric and stratospheric waves. - *Scientific Technical Report STR 04/18* (2004), http://bib.gfz-potsdam.de/pub/str0418/0418.pdf.

Pauli W. The Influence of Archetypal Ideas on the Scientific Theories of Kepler. - In: Two Lectures given by Professor W. E. Pauli, in 1948, at the Psychological Club of Zurich. https://docshare.tips/the-influence-of-archetypal-ideas-on-the-scientific-theories-of-kepler_5860709ab6d87fabad8b70aa.html

Petoukhov S.V. *Matrix genetics, algebras of genetic code, noise immunity*. Moscow, RCD, 316 p. (2008a, in Russian). ISBN 978-5-93972-643-6.

Petoukhov S.V. The system-resonance approach in modeling genetic structures. – *Biosystems*, January 2016, v. 139, p. 1-11. http://dx.doi.org/10.1016/j.biosystems.2015.11.001, http://petoukhov.com/PETOUKHOV_ARTICLE_IN_BIOSYSTEMS.pdf.

Petoukhov S.V. Nucleotide Epi-Chains and New Nucleotide Probability Rules in Long DNA Sequences. Preprints 2019, 2019040011, 17 pages, (2019), DOI: 10.20944/preprints201904.0011.v1, https://www.preprints.org/manuscript/201904.0011/v1

Petoukhov S.V. Hyperbolic Rules of the Cooperative Organization of Eukaryotic and Prokaryotic Genomes. *Biosystems*, 198, 104273 (2020a).

Petoukhov S.V. Hyperbolic Rules of the Oligomer Cooperative Organization of Eukaryotic and Prokaryotic Genomes. *Preprints* 2020, 2020050471 (2020b), doi:10.20944/preprints202005.0471.v2, https://www.preprints.org/manuscript/202005.0471/v2.

Petoukhov S.V. The rules of long DNA-sequences and tetra-groups of oligonucleotides. arXiv:1709.04943v6 , 6th version from 22.05.2020 (2020c).

Preprints (www.preprints.org) | NOT PEER-REVIEWED | Posted: 26 April 2022   doi:10.20944/preprints202203.0100.v2

Petoukhov S.V. Algebraic Rules for the Percentage Composition of Oligomers in Genomes. *Preprints* **2021**, 2021010360 (2021a), 84 pages (DOI: 10.20944/preprints202101.0360.v3).

Petoukhov S.V. Modeling inherited physiological structures based on hyperbolic numbers, *BioSystems*, Vol. 199, 104285 (2021b), ISSN 0303-2647, https://doi.org/10.1016/j.biosystems.2020.104285.

Petoukhov S.V. Algebraic harmony and probabilities in genomes. Long-range coherence in quantum code biology.- *Biosystems*, Vol. 209, 104503 (2021c).

Petoukhov S.V., He M. *Symmetrical Analysis Techniques for Genetic Systems and Bioinformatics: Advanced Patterns and Applications*. Hershey, USA, IGI Global (2010). http://www.evernote.com/l/AFnRwSleQRRMI7PGAKFzZgkUEdMP10Lv5J0/

Petoukhov S.V., Petukhova E.S., Svirin V.I. Symmetries of DNA alphabets and quantum informational formalisms. *Symmetry: Culture and Science,* Vol. 30, No. 2, p.161-179 (2019), https://doi.org/10.26830/symmetry_2019_2_161.

Petoukhov S.V., Svirin V.I., Khazina L.V. Bionics of spiral structures. *Journal of Machinery Manufacture and Reliability*, Vol. 44, No. 3, pp. 249–253 (2015).

Planck M. Scientific ideas, their origin, and effects. In: Planck M. (Ed.), *The Philosophy of Physics*. W.W. Norton & Company, USA (1936).

Prigg M. Stunning image shows diver through the 'eyes' of a DOLPHIN and reveals animals send images through water to each other. Daily *Mail* (4 December 2015), https://www.dailymail.co.uk/sciencetech/article-3346588/What-dolphins-REALLY-Stunning-image-shows-diver-eyes-mammal-reveals-animals-send-images-water-other.html].

Ryapolov A.V., Fambulov N.V. Anti-jamming antenna array model for satellite navigation equipment. *Journal of «Almaz–Antey» Air and Space Defence Corporation*., 3, 20-29 (2018). https://doi.org/10.38013/2542-0542-2018-3-20-29

Sazonov D.M. *Multi-element antenna systems. Matrix approach*. - Moscow, Radiotechnika (2015). ISBN 978-5-93-108-093-2 (in Russian).

Schakenraad K., Ernst J., Pomp W., Danen E. H. J.,. Merks R. M. H, Schmidt T., Giomi L. *Soft Matter*, 16, 6328 (2020)].

Schrödinger E. *What is life?* Cambridge Press (1944).

Shishkin G.G., Shishkina A.G. Electronics. M., Drofa. 2009 (in Russian).

Sluckin T.J., Dunmur D.A., Stegemeyer H. *Crystals That Flow: Classic Papers from the History of Liquid Crystals*. **-** Taylor & Francis, p.738, 2004, ISBN 0415257891, 9780415257893; https://en.wikipedia.org/wiki/Liquid_crystal

Slyusar V.I. New Matrix Operations for Digital Signal Processing. – *Projects: Multidimensional signal processing for digital antenna arrays. Tensor-matrix theory of Artificial Intelligence* (November 1999). DOI: 10.13140/RG.2.2.31620.76164/1

Slyusar V.I. Nanoantennas: Approaches and Prospects. // *Electronics: Science, Technology, Business*. № 2, p. 58-65 (2009, in Russian).

Slyusar V.I. Wireless networks on a crystal. - *Electronics: Science, Technology, Business*, №6 (00112), p. 74-83 (2011, in Russian), https://www.slyusar.kiev.ua/ENTB_06_2011_074_083.pdf

Slyusar V.I. Tensor-matrix theory of artificial intelligence. - Preprint for 63rd All-Russian Scientific Conference of MIPT. November 23-29, 2020 (August 2020, in Russian), DOI: 10.13140/RG.2.2.24685.41448, https://www.researchgate.net/publication/348804997_Tenzorno-matricnaa_teoria_iskusstvennogo_intellekta.

Slyusar V.I. Key aspects of the tensor-matrix theory of analysis and processing of multichannel measuring signals in the classical and neural network approaches. – Presentation at the 10th International Symposium on Precision Mechanical Measurement, Qingdao, China, VTC, p.1-46 (October 2021). DOI: 10.13140/RG.2.2.31722.64966/1

Slyusar V. Neural Networks Models based on the tensor-matrix theory. (August 2021). DOI: 10.31114/2078-7707-2021-2-23-28.

Solomatin V. Faceted vision: perspectives in optoelectronic systems. *Photonics*, №1, p. 22-25 (2001).

Stewart I. *Life's other secret: The new mathematics of the living world*. N.-Y.: Penguin (1999).

Stutzman W.L.; Thiele G. A. Antenna Theory and Design. John Wiley & Sons (2012). ISBN 978-0470576649.

Teyssier J., Saenko S.V., van der Marel D., Milinkovitch M.C. Photonic Crystals Cause Active Colour Change in Chameleons. *Nature communications*, 6, 6368 (2015)].

Voskresensky D.I., Gostyukhin V.L., Maksimov V.M., Ponomarev L.I. Microwave devices and antennas. M., Radiotechnika, 2006 (in Russian).

Wensink H.H., Dunkel J., Heidenreich S., Drescher K., Goldstein R.E., Löwen H., Yeomans J.M. Meso-scale turbulence in living fluids. *Proceedings of the National Academy of Sciences of the United States of America*. **109** (36): 14308–13 (2012). doi:10.1073/pnas.1215368110. PMC 3607014. PMID 22908244

Yevdokimov Yu. M. Nucleic acids, liquid crystals, and secrets of nanodesign. *Science and Life*, No. 4 (2005), https://www.nkj.ru/archive/articles/604/.

Yevdokimov Yu. M., Skuridin S. G., Salyanov V. I., Bykov V.A., Palumbo M. *Structural DNA Nanotechnology: Liquid-Crystalline Approach* (Transworld **Research Network), 2012, http://www.trnres.com/ebook.php**

Yuste R., Levin M. New Clues about the Origins of Biological Intelligence. - *Scientific American* (December 2021). https://www.scientificamerican.com/article/new-clues-about-the-origins-of-biological-intelligence/

Zabeo D., Heumann J.M., Schwartz C.L., Suzuki-Shinjo A., Morgan G., Widlund P.O., Höög J.L.A lumenal interrupted helix in human sperm tail microtubules. Scientific Reports, 8(1), 2727 (2018 Feb 9) DOI: 10.1038/s41598-018-21165-8. PMID.29426884; PMCID: PMC5807425.

Zaitsev D.F. *Nanophotonics and its applications*. – Moscow, firm "Aktion", 427 p. (2011, in Russian). https://www.studmed.ru/zaycev-d-f-nanofotonika-i-ee-primenenie_96c07b57122.html.